Multi-Kingdom Biofilms Breached: Microneedle Delivery of Metabolically Targeted Organic Silver–Photosensitizers for Polymicrobial Infections in Diabetic Foot Ulcers

Haohan Li, [a,b] Xiaohui Liu, [c] Can Hou [d] *, Duoyang Fan, [a,b] Xiang Cheng, [a,b] Ying Chen, [a,b] Jie Dong, [a,b] Wenbin Zeng, [a,b] * Fei Chen, [a,b] *

[a] *Xiangya School of Pharmaceutical Sciences, Central South University, Changsha 410013, China*

[b] *Hunan Key Laboratory of Diagnostic and Therapeutic Drug Research for Chronic Diseases, Changsha 410013, China*

[c] *The Affiliated Nanhua Hospital, Hengyang Medical School, University of South China, Hengyang 421000, China*

[d] *National Clinical Research Center for Endocrine and Metabolic Diseases, Department of Metabolism and Endocrinology, the Second Xiangya Hospital, Central South University, Changsha 410013, China*

[*] *Corresponding author.*

E-mail addresses: fechen@csu.edu.cn; wbzeng@csu.edu.cn; houcan84@csu.edu.cn.

Haohan Li and Xiaohui Liu contributed equally to this work.

Experimental Sections

Syntheses and Characterizations

Synthesis of intermediate compound 1. A solution containing 4-(diphenylamino) phenylboronic acid (1156 mg, 4.00 mmol), 4,7-dibromo-2,1,3-benzothiadiazole (1176 mg, 4.00 mmol), K_2CO_3 (200 mg) and $Pd(dppf)Cl_2$ (20 mg) in THF (5 mL) and MeOH (10 mL) was heated to reflux under a nitrogen atmosphere for 8 h. After the reaction was completed, the mixture was allowed to cool to room temperature and subsequently poured into water. The aqueous phase was extracted with dichloromethane (DCM), and the combined organic layers were dried over anhydrous Na_2SO_4 and concentrated under reduced pressure. The crude product was purified by silica gel column chromatography (petroleum ether/DCM) to afford Compound 1 as an orange solid (1005 mg, 55% yield). **^{1}H NMR** (500 MHz, DMSO-d_6) δ 8.09 (d, J = 7.6 Hz, 1H), 7.93 – 7.89 (m, 2H), 7.74 (d, J = 7.6 Hz, 1H), 7.40 – 7.32 (m, 4H), 7.15 – 7.05 (m, 8H).

Synthesis of intermediate compound TPAM. Compound **1** (500 mg, 1.11 mmol) was combined with imidazole (150 mg, 2.21 mmol), K_2CO_3 (287 mg, 2.08 mmol), and $CuSO_4 \cdot 5H_2O$ (80 mg, 0.32 mmol) in DMF (6 mL). The mixture was heated at 120 °C with stirring for 10 h. After cooling, the reaction was poured into water and extracted with ethyl acetate (EA). The organic layer was dried over anhydrous Na_2SO_4 and concentrated under reduced pressure. Purification by silica-gel column chromatography (DCM/methanol) afforded Compound **TPAM** as a red solid (260 mg, 56% yield). **^{1}H NMR** (500 MHz, $CDCl_3$) δ 8.46 (s, 1H), 7.84 (d, J = 8.8 Hz, 2H), 7.78 – 7.72 (m, 2H), 7.66 (d, J = 7.6 Hz, 1H), 7.34 – 7.27 (m, 5H), 7.24 – 7.16 (m, 6H), 7.09 (tt, J = 7.2, 1.2 Hz, 2H).

Synthesis of compound T-C_{12}. TPAM (200 mg, 0.44 mmol) was combined with 1-bromododecane (250 mg, 1.0 mmol) in DMF (4 mL). The mixture was heated at 100 °C under stirring for 10 h to promote quaternization. After the reaction reached completion, the mixture was poured into water to terminate the process, followed by extraction with ethyl acetate. The combined organic phases were dried over anhydrous Na_2SO_4 and concentrated under reduced pressure. The crude product was then purified

by silica gel column chromatography using a DCM/methanol eluent system to afford **T-C_{12}** as a red solid (199.5 mg, yield: 70%). **^{1}H NMR** (500 MHz, $CDCl_3$) δ 10.11 (s, 1H), 8.52 (t, J = 1.9 Hz, 1H), 8.26 (d, J = 7.8 Hz, 1H), 8.20 (t, J = 1.8 Hz, 1H), 8.08 (d, J = 7.7 Hz, 1H), 8.04 – 7.96 (m, 2H), 7.43 – 7.33 (m, 4H), 7.20 – 7.08 (m, 8H), 4.39 (t, J = 7.2 Hz, 2H), 1.94 (p, J = 7.8 Hz, 2H), 1.40 – 1.15 (m, 21H). **^{13}C NMR** (126 MHz, $CDCl_3$) δ 154.11, 149.11, 147.10, 136.99, 136.02, 130.19, 129.49, 126.61, 125.35, 124.45, 123.86, 123.36, 123.01, 122.53, 122.05, 121.98, 77.30, 77.05, 76.79, 50.86, 31.89, 30.31, 29.59, 29.50, 29.39, 29.39, 29.31, 29.05, 26.33, 22.67, 14.10.

Synthesis of intermediate compound T-NH-Boc and T-NH_2. Compound **TPAM** (200 mg, 0.44 mmol) was combined with tert-Butyl (6-bromohexyl) carbamate (150 mg, 0.53 mmol) in DMF (4 mL). The mixture was heated at 120 °C with stirring for 10 h. After cooling, the reaction was poured into water and extracted with EA. The organic layer was dried over anhydrous Na_2SO_4 and concentrated under reduced pressure. Purification by silica-gel column chromatography (DCM/methanol) afforded Compound **T-NH-Boc** as a red solid (263 mg, 87% yield). Then, the crude **T-NH-Boc** was dissolved in DCM (2 mL), followed by the addition of trifluoroacetic acid (0.5 mL). The mixture was stirred at room temperature until complete removal of the Boc group. The reaction was then neutralized with saturated $NaHCO_3$ solution and extracted with DCM/water. The red organic phase was collected, dried, evaporated, and further purified by HPLC to afford **T-NH_2** as a red solid (189 mg, 84% yield). **^{1}H NMR** (500 MHz, DMSO-d_6) δ 10.07 (s, 1H), 8.55 – 8.49 (m, 1H), 8.25 (d, J = 7.7 Hz, 1H), 8.18 (d, J = 1.9 Hz, 1H), 8.08 (d, J = 7.8 Hz, 1H), 8.03 – 7.98 (m, 2H), 7.39 (t, J = 7.9 Hz, 4H), 7.14 (dt, J = 8.8, 6.3 Hz, 8H), 4.39 (t, J = 7.2 Hz, 2H), 2.80 (s, 2H), 1.93 (p, J = 7.2 Hz, 2H), 1.56 (q, J = 7.4 Hz, 2H), 1.37 (dt, J = 9.6, 5.6 Hz, 4H).

Synthesis of compound T-BOB. T-NH_2 (120 mg, 0.19 mmol), 1-hydroxy-1,3-dihydrobenzo[c] [1,2] oxaborole-5-carboxylic acid (53.4 mg, 0.30 mmol) and HATU (80 mg, 0.20 mmol) were dissolved in DMF (5 mL). N, N-Diisopropylethylamine (0.7 mg, 0.005 mmol) was added dropwise, and the mixture was stirred at room temperature for 12 h. After completion, the reaction mixture was diluted with water and extracted with ethyl acetate, followed by a second extraction with water. Removal of the solvent

under reduced pressure afforded a residue that was purified by HPLC to give **T-BOB** as a red solid (89 mg, 52% yield). **^{1}H NMR** (500 MHz, DMSO-d_6) δ 10.05 (s, 1H), 9.33 (s, 1H), 8.23 (d, J = 7.8 Hz, 1H), 8.17 (t, J = 1.8 Hz, 1H), 8.07 (d, J = 7.7 Hz, 1H), 8.03 – 7.96 (m, 2H), 7.85 – 7.79 (m, 1H), 7.76 (d, J = 1.1 Hz, 2H), 7.43 – 7.35 (m, 4H), 7.19 – 7.06 (m, 8H), 5.76 (s, 1H), 5.02 (s, 2H), 4.38 (t, J = 7.2 Hz, 2H), 3.29 – 3.20 (m, 2H), 1.94 (d, J = 8.0 Hz, 2H), 1.56 (q, J = 7.0 Hz, 2H), 1.39 (p, J = 4.0, 3.5 Hz, 4H). **^{13}C NMR** (126 MHz, DMSO-d_6) δ 166.75, 154.35, 153.65, 148.80, 148.69, 147.16, 137.41, 137.30, 134.80, 130.93, 130.76, 130.24, 129.43, 126.81, 126.23, 125.28, 124.91, 124.74, 124.40, 123.43, 123.39, 122.28, 120.47, 70.36, 55.37, 49.97, 40.51, 40.34, 40.17, 40.01, 39.84, 39.67, 39.51, 29.69, 29.36, 26.30, 25.74. **HRMS** (m/z): calculated for $C_{41}H_{38}BN_6OS^+$ $[M]^+$: 705.2814; found: 705.2821.

Synthesis of intermediate compound T-CCH. Compound **TPAM** (200 mg, 0.44 mmol) was mixed with 6-bromohex-1-yne (90 mg, 0.55 mmol) in DMF (4 mL). The reaction mixture was heated to 120 °C and kept under stirring for 10 h. After being allowed to cool to room temperature, the mixture was poured into water and extracted with DCM. The combined organic phase was dried over anhydrous Na_2SO_4 and concentrated under reduced pressure. The crude product was purified by silica-gel column chromatography (DCM/methanol) to afford **T-CCH** as a red solid (211 mg, 89% yield). **^{1}H NMR** (500 MHz, DMSO-d_6) δ 10.07 (s, 1H), 8.52 (t, J = 1.9 Hz, 1H), 8.25 (d, J = 7.7 Hz, 1H), 8.18 (t, J = 1.8 Hz, 1H), 8.09 (d, J = 7.8 Hz, 1H), 8.04 – 7.97 (m, 2H), 7.42 – 7.34 (m, 4H), 7.18 – 7.10 (m, 8H), 4.42 (t, J = 7.1 Hz, 2H), 2.84 (t, J = 2.6 Hz, 1H), 2.28 (td, J = 7.1, 2.7 Hz, 2H), 2.07 – 1.99 (m, 2H), 1.55 (dq, J = 10.0, 7.1 Hz, 2H).

Synthesis of compound T-DAla. Compound **T-CCH** (30 mg, 0.06 mmol) and 3-azido-D-alanine·HCl (8 mg, 0.05 mmol) were dissolved in a THF/H_2O mixture (2:1, v/v, 2 mL). $CuSO_4$ (2.50 mg, 0.01 mmol) and vitamin C (17.6 mg, 0.10 mmol) were then added, and the reaction mixture was stirred at 50 °C under nitrogen in the dark for 8 h. After completion, the solvent was removed under reduced pressure, and the residue was purified by HPLC. Lyophilization of the collected fractions afforded **T-DAla** as a red solid (26 mg, 60% yield). **^{1}H NMR** (500 MHz, $CDCl_3$) δ 10.89 (s, 1H), 8.42 (s, 2H),

7.84 (d, J = 8.5 Hz, 3H), 7.62 (s, 1H), 7.31 (t, J = 7.7 Hz, 4H), 7.23 – 7.02 (m, 9H), 4.57 (s, 2H), 2.30 (s, 2H), 2.16 (s, 2H), 1.99 (d, J = 2.5 Hz, 1H), 1.62 (s, 2H), 1.27 (dd, J = 12.2, 3.7 Hz, 4H). **^{13}C NMR** (101 MHz, $CDCl_3$) δ 154.12, 149.14, 148.01, 147.11, 137.75, 136.20, 130.22, 129.75, 129.49, 128.62, 126.48, 125.34, 124.14, 123.86, 123.47, 122.79, 122.09, 121.91, 83.07, 77.36, 77.04, 76.72, 69.56, 50.22, 29.70, 29.32, 29.09, 24.77, 22.68, 17.82, 14.11. **HRMS** (m/z): calculated for $C_{36}H_{34}N_9O_2S^+$ $[M]^+$: 656.2551 and $C_{36}H_{35}N_9O_2S^{2+}$ $[M]^{2+}$: 328.6312; found:656.2521 and 328.6322.

Synthesis of compound T-C_{12}-Ag, T-BOB-Ag, T-DAla-Ag. Compound (**T-C_{12}**, **T-BOB** or **T-DAla**) was dissolved in dry DCM, followed by the addition of Ag_2O. The mixture was stirred at room temperature in the dark for 12 h. After completion, the suspension was filtered through Celite, and the filtrate was concentrated under reduced pressure. **T-C_{12}-Ag**: **^{1}H NMR** (500 MHz, $CDCl_3$) δ 8.11 (d, J = 39.5 Hz, 1H), 7.80 (d, J = 8.3 Hz, 2H), 7.71 (d, J = 20.5 Hz, 2H), 7.29 (t, J = 7.8 Hz, 4H), 7.18 (d, J = 8.2 Hz, 7H), 7.07 (t, J = 7.3 Hz, 3H), 4.23 (s, 2H), 1.89 (s, 2H), 1.25 (d, J = 8.4 Hz, 18H), 0.88 (d, J = 6.8 Hz, 4H). **^{13}C NMR** (126 MHz, $CDCl_3$) δ 158.41, 153.55, 153.43, 151.90, 142.22, 139.53, 135.71, 135.59, 135.00, 134.98, 134.17, 131.64, 131.51, 130.02, 129.63, 129.43, 129.13, 128.30, 128.06, 127.02, 54.73, 45.69, 45.28, 45.11, 44.95, 44.78, 44.61, 44.45, 44.28, 36.50, 34.50, 34.25, 34.23, 34.16, 34.06, 33.92, 33.60, 30.76, 27.30, 19.16. **T-BOB-Ag**: **^{1}H NMR** (400 MHz, $CDCl_3$) δ 8.01 – 7.91 (m, 1H), 7.84 (d, J = 8.7 Hz, 2H), 7.75 (d, J = 7.6 Hz, 1H), 7.68 (d, J = 1.9 Hz, 1H), 7.35 – 7.26 (m, 7H), 7.24 – 7.15 (m, 7H), 7.13 – 7.03 (m, 3H), 5.29 (s, 2H), 4.66 (s, 1H), 4.26 (t, J = 7.3 Hz, 2H), 3.43 (q, J = 6.9 Hz, 2H), 1.69 – 1.60 (m, 2H), 1.48 (s, 2H), 1.30 – 1.20 (m, 4H). **^{13}C NMR** (101 MHz, $CDCl_3$) δ 176.74, 165.69, 160.73, 152.21, 148.29, 146.92, 145.32, 145.17, 139.64, 133.33, 133.03, 128.30, 128.22, 127.70, 127.59, 127.55, 127.35, 127.27, 126.64, 124.44, 124.33, 123.42, 123.31, 121.97, 121.79, 121.45, 120.43, 120.14, 119.45, 114.49, 75.45, 75.13, 74.82, 62.71, 51.54, 50.45, 37.81, 28.95, 27.80, 27.42, 27.18, 24.06, 23.64. **T-DAla-Ag**: **^{1}H NMR** (400 MHz, $CDCl_3$) δ 7.56 (s, 6H), 7.25 – 7.15 (m, 4H), 7.15 – 6.50 (m, 9H), 4.31 (s, 2H), 2.99 (s, 2H), 2.09 – 1.87 (m, 3H), 1.32 – 1.23 (m, 4H). **^{13}C NMR** (101 MHz, $CDCl_3$) δ 147.60, 146.13, 129.00, 128.72, 128.40, 124.06, 122.61, 76.31, 76.00, 75.68, 30.89, 28.68, 28.50, 28.30,

28.22, 26.20, 21.67, 13.10.

Supplementary Figures and Tables

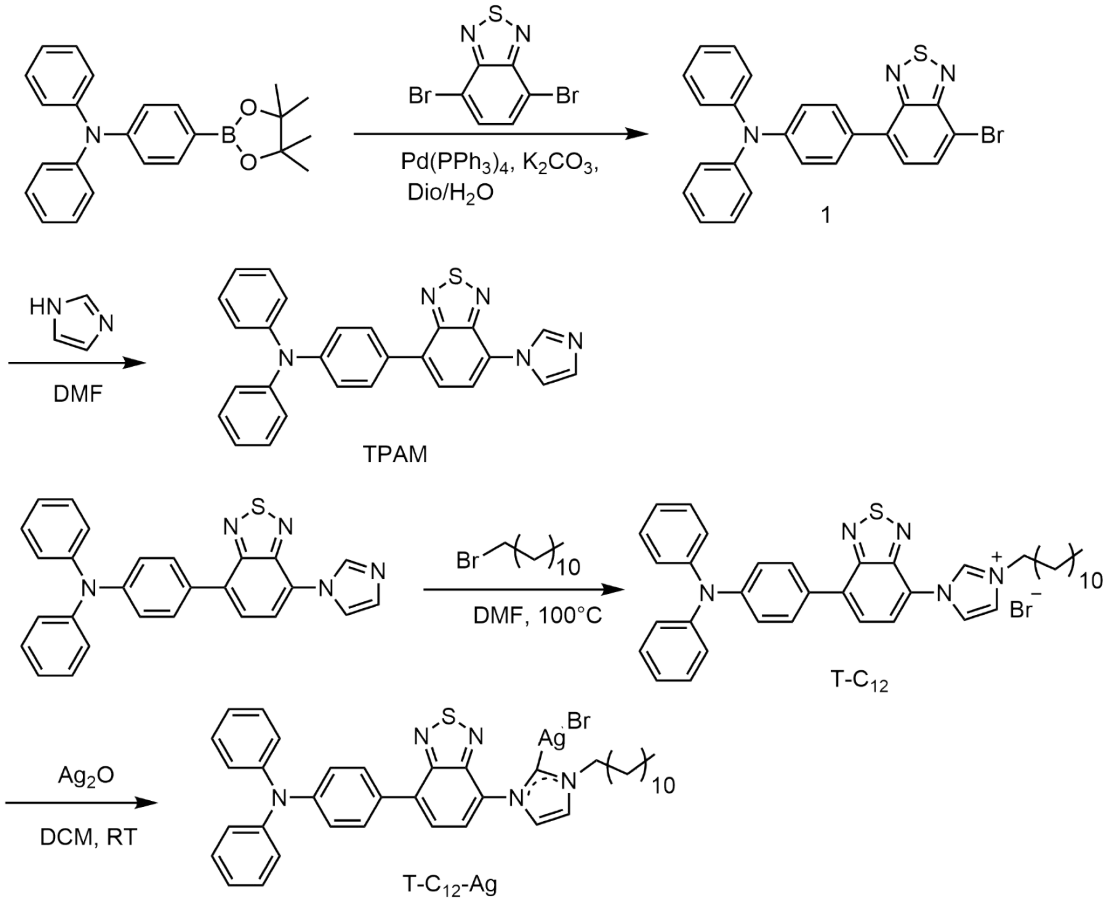

Figure S1. Synthetic route and chemical structures of **T-C_{12}** and **T-C_{12}-Ag**.

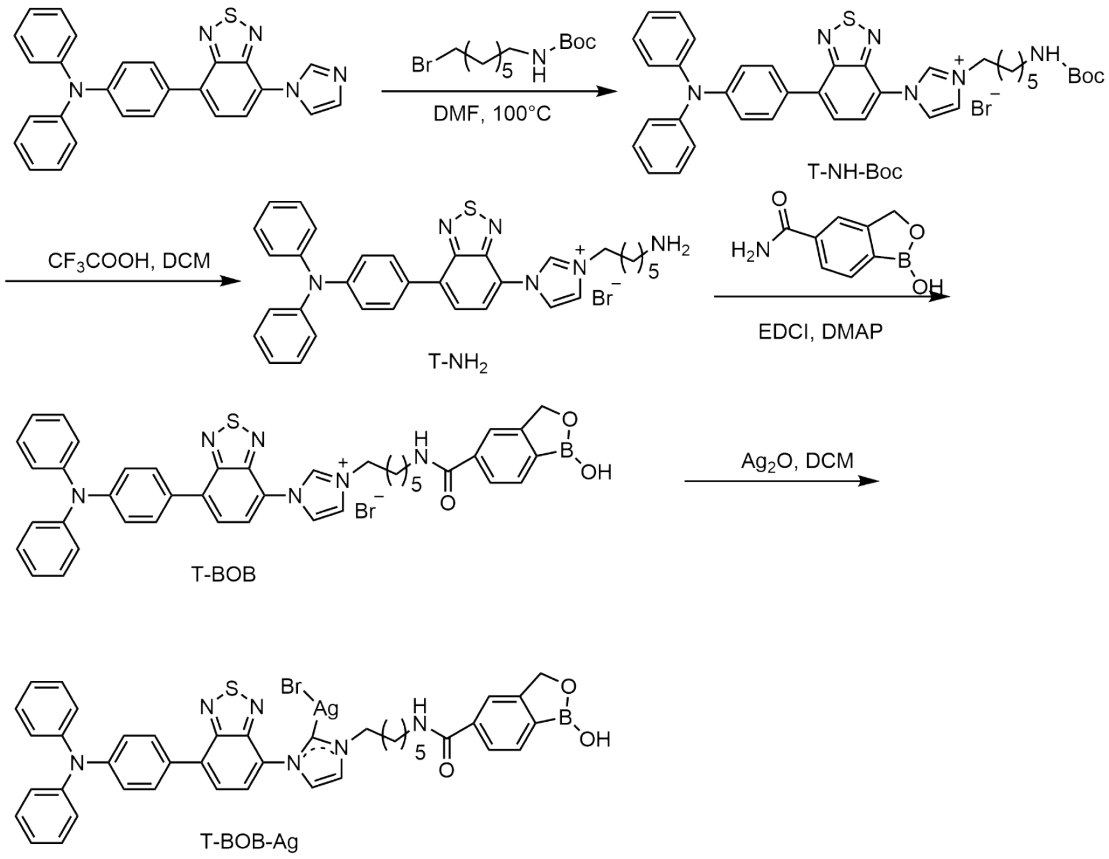

Figure S2. Synthetic route and chemical structures of **T-BOB** and **T-BOB-Ag**.

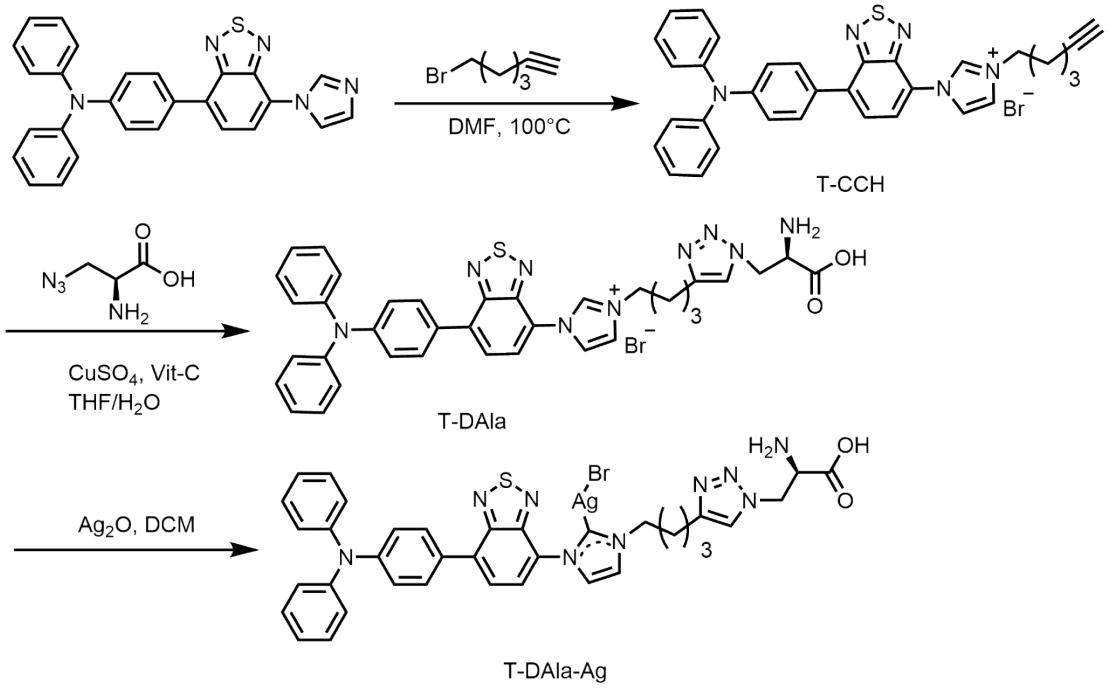

Figure S3. Synthetic route and chemical structures of **T-DAla** and **T-DAla-Ag**.

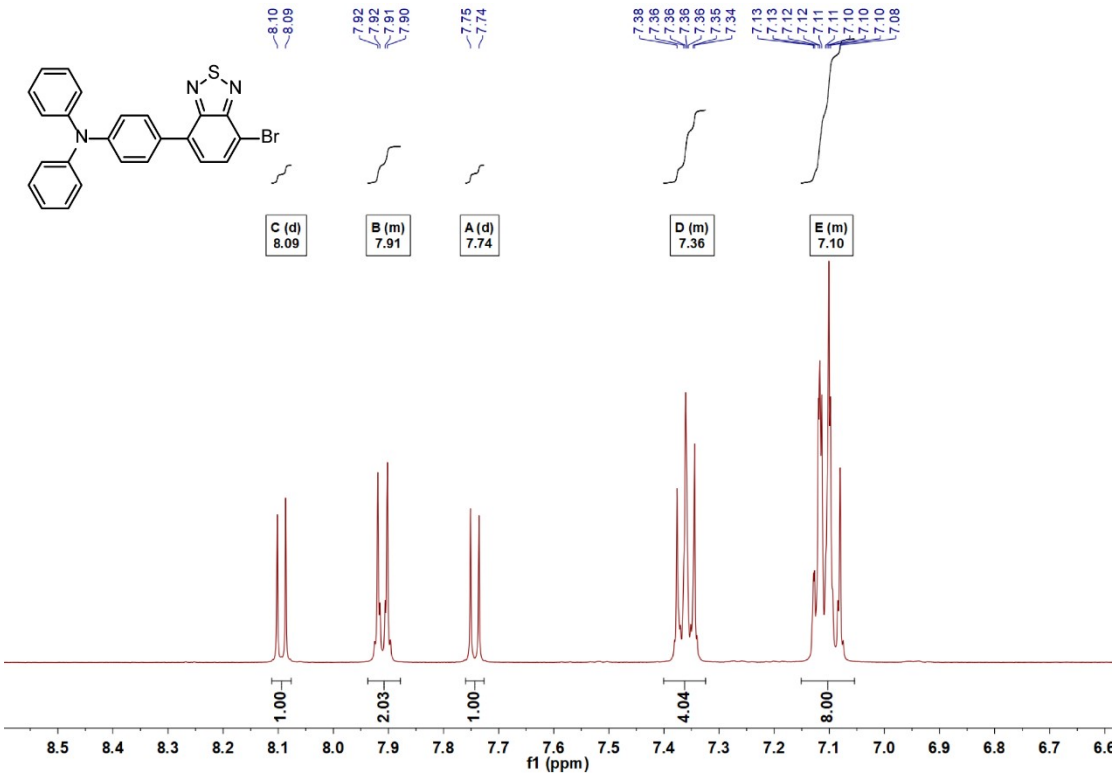

Figure S4. [1]H NMR spectrum of compound **1**.

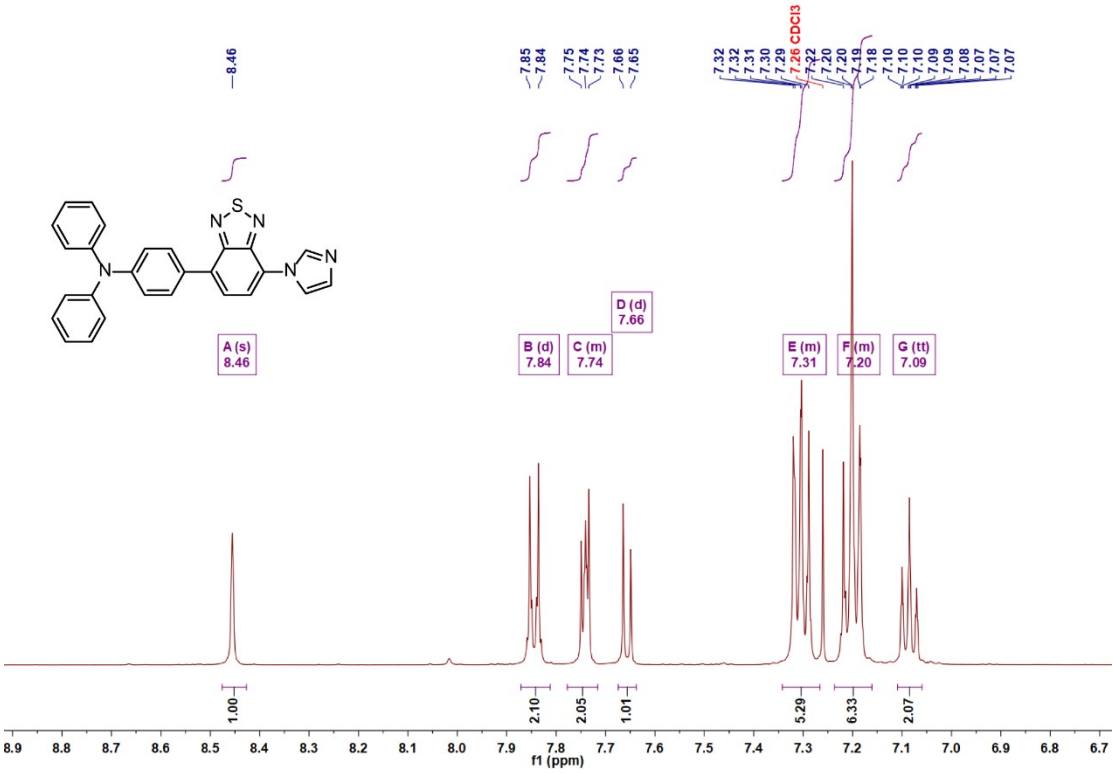

Figure S5. [1]H NMR spectrum of compound **TPAM**.

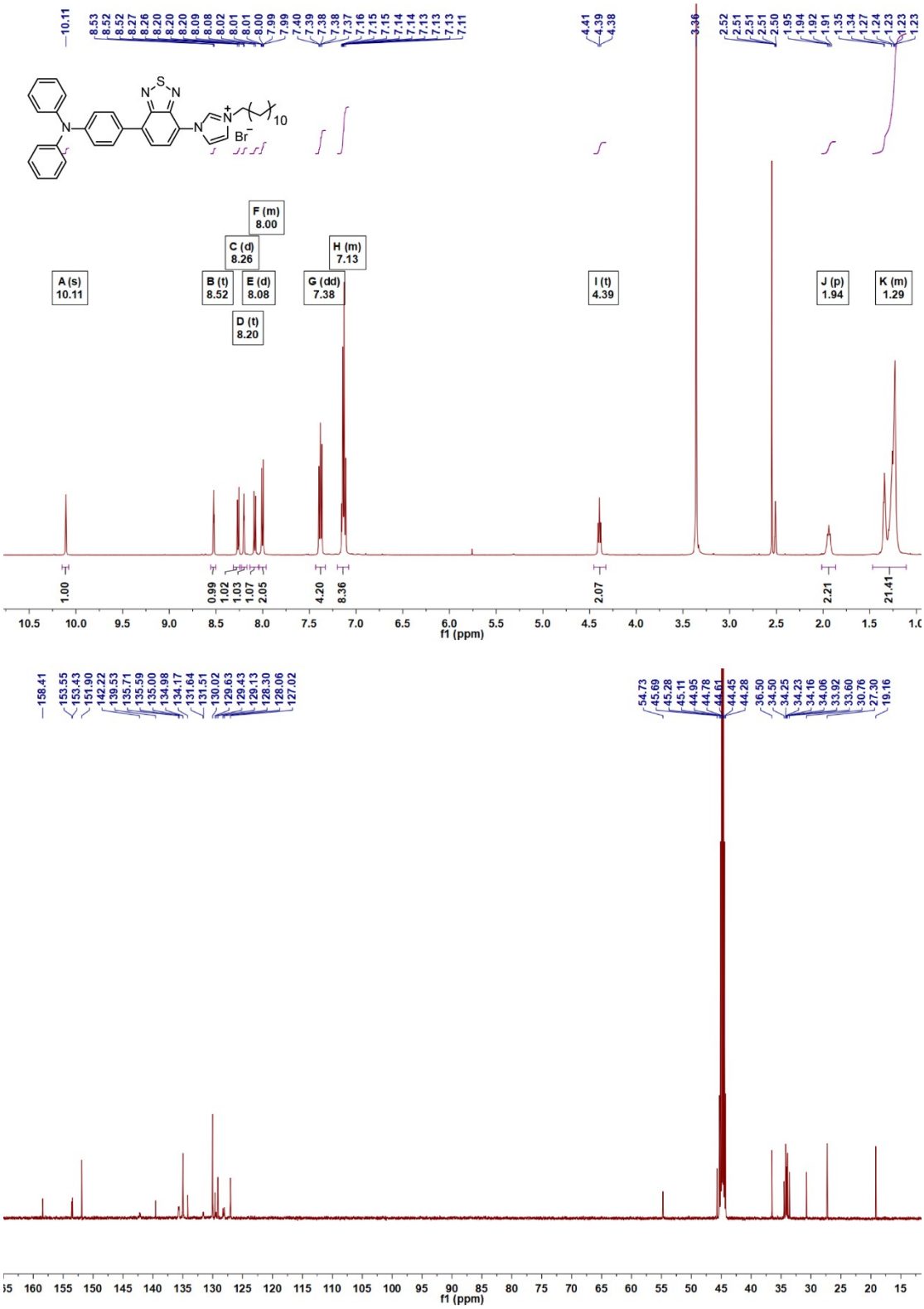

Figure S6. ^{1}H NMR and ^{13}C NMR spectrum of compound **T-C_{12}**.

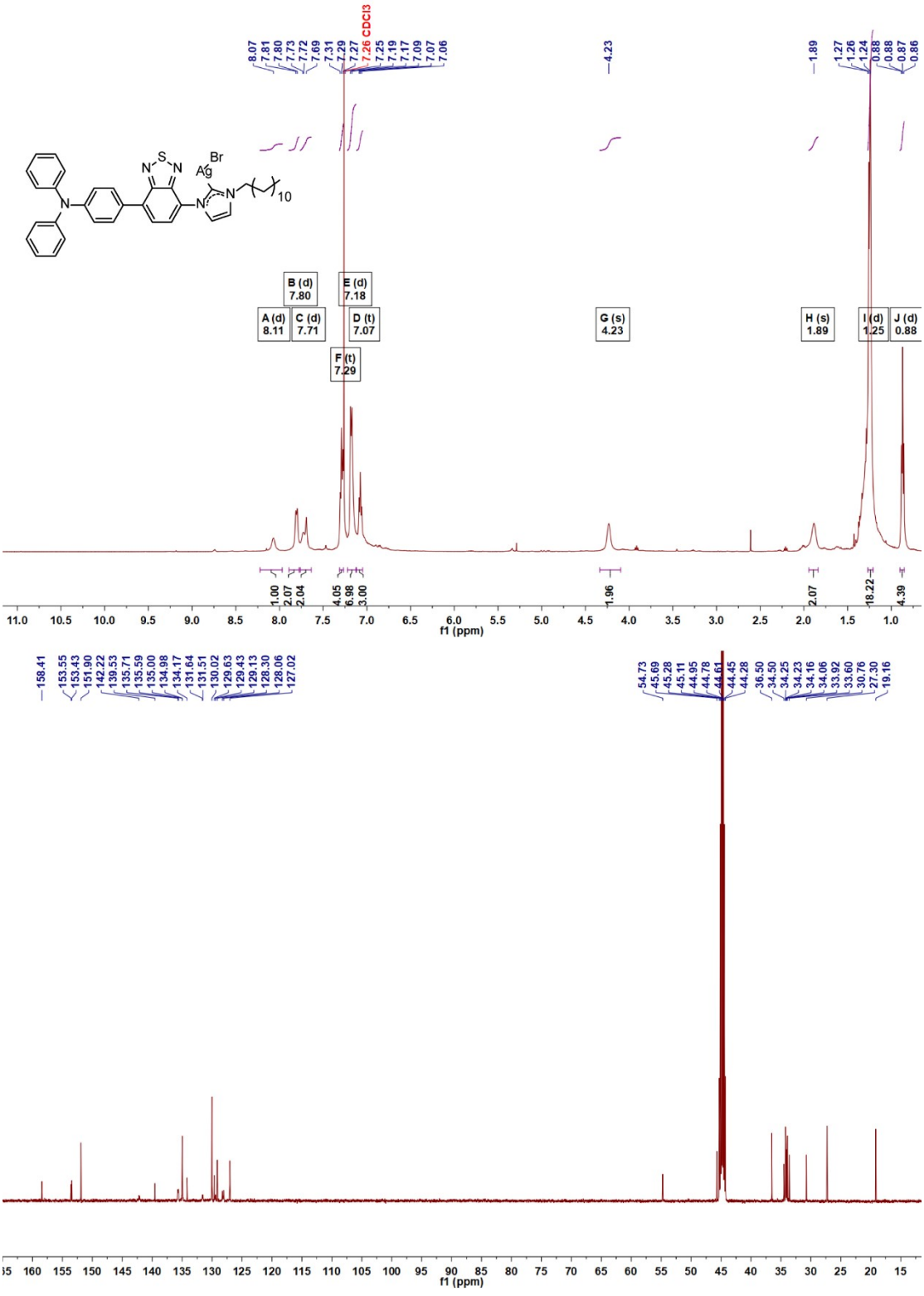

Figure S7. ^{1}H NMR and ^{13}C NMR spectrum of compound **T-C_{12}-Ag**.

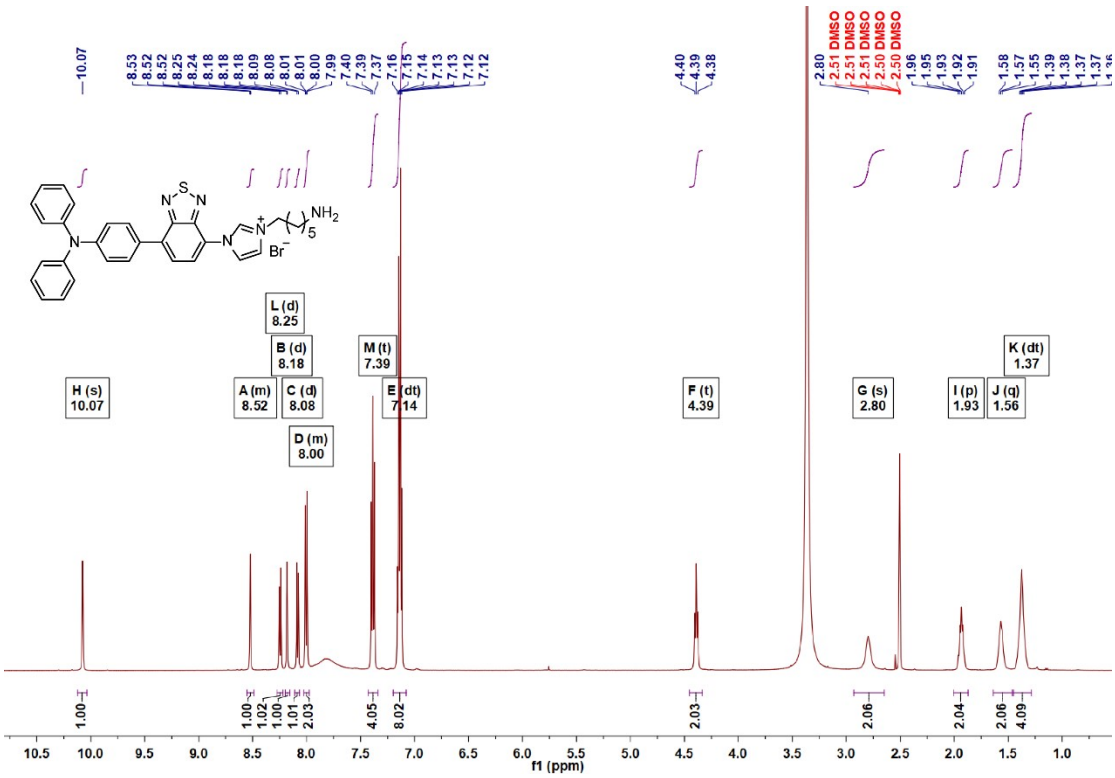

Figure S8. ^{1}H NMR spectrum of compound **T-NH$_2$**.

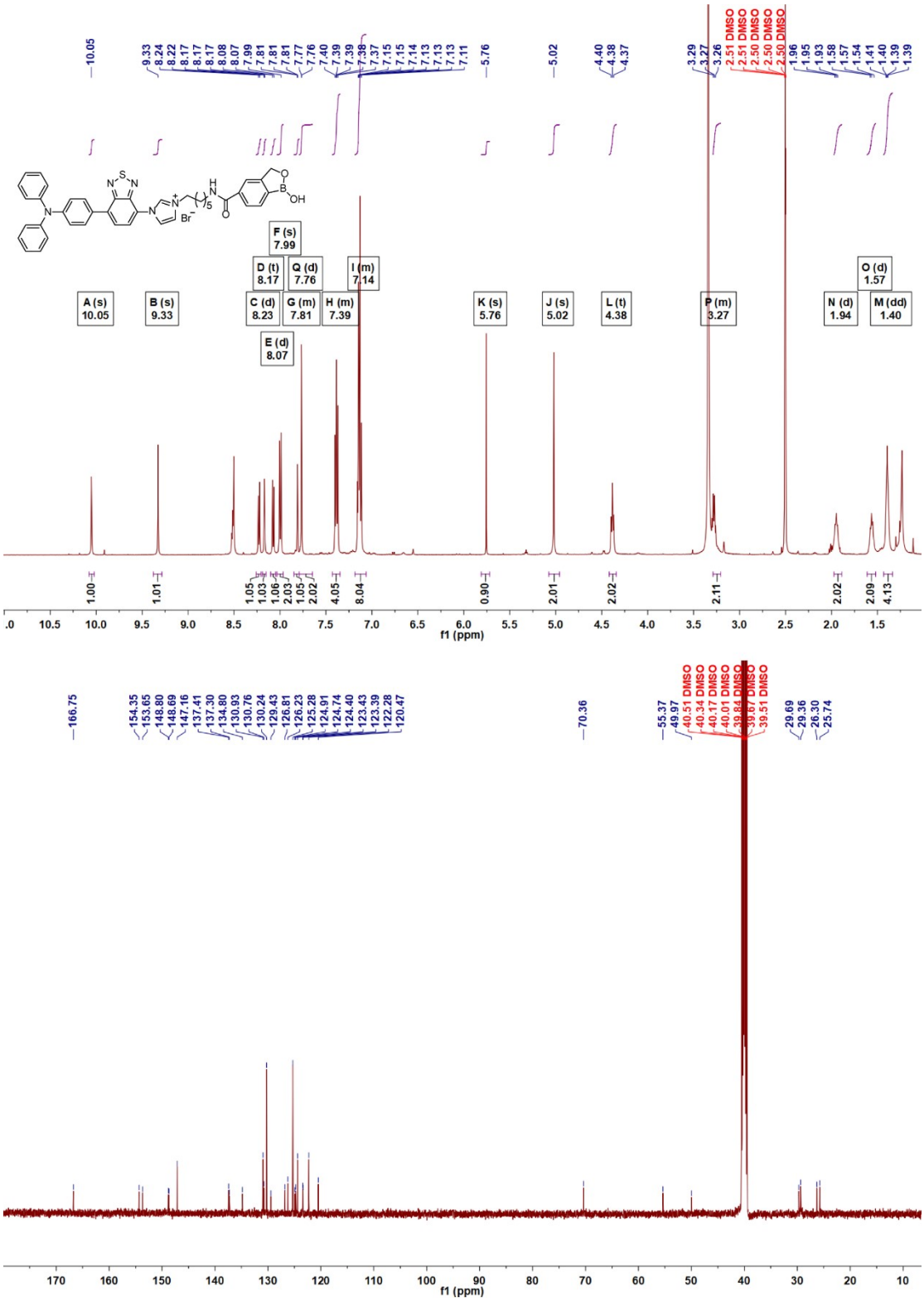

Figure S9. ^{1}H NMR and ^{13}C NMR spectrum of compound **T-BOB**.

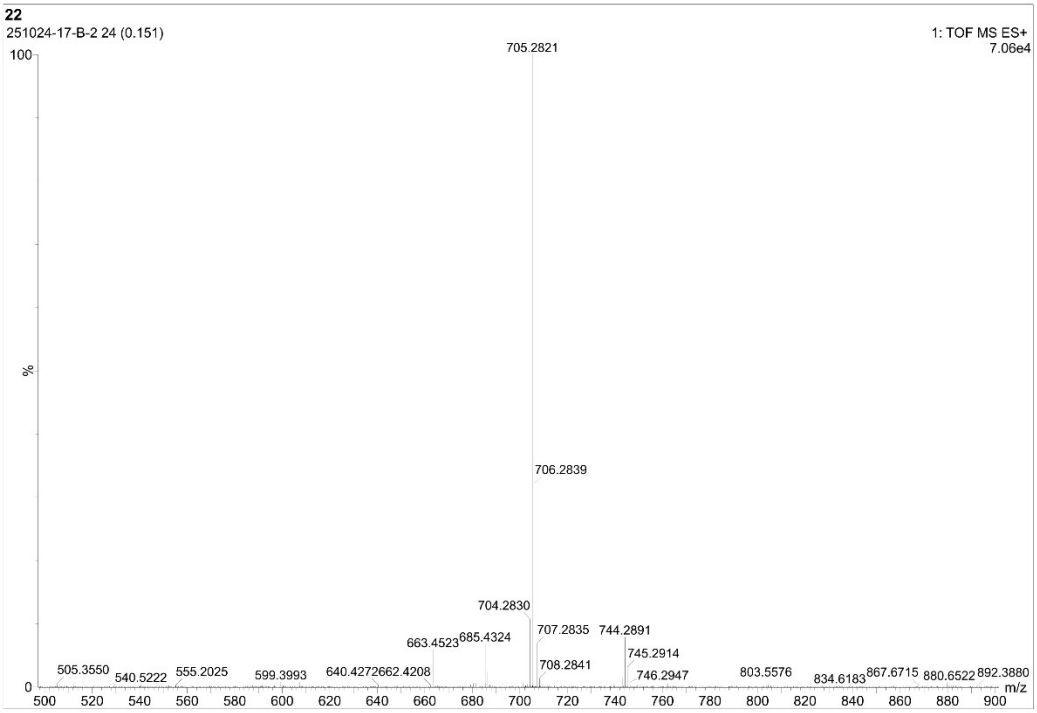

Figure S10. HRMS spectrum of compound **T-BOB**.

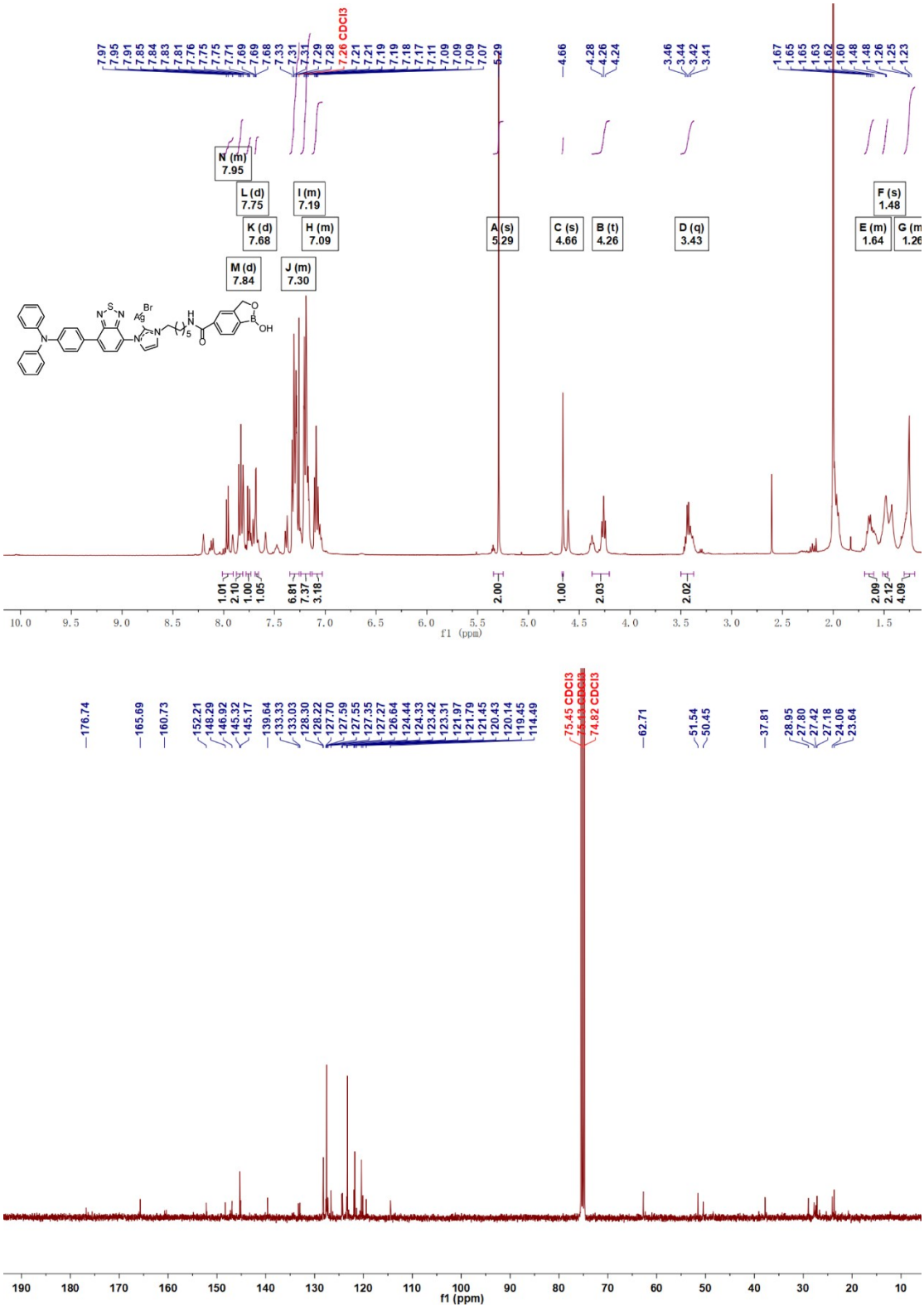

Figure S11. ^{1}H NMR and ^{13}C NMR spectrum of compound **T-BOB-Ag**.

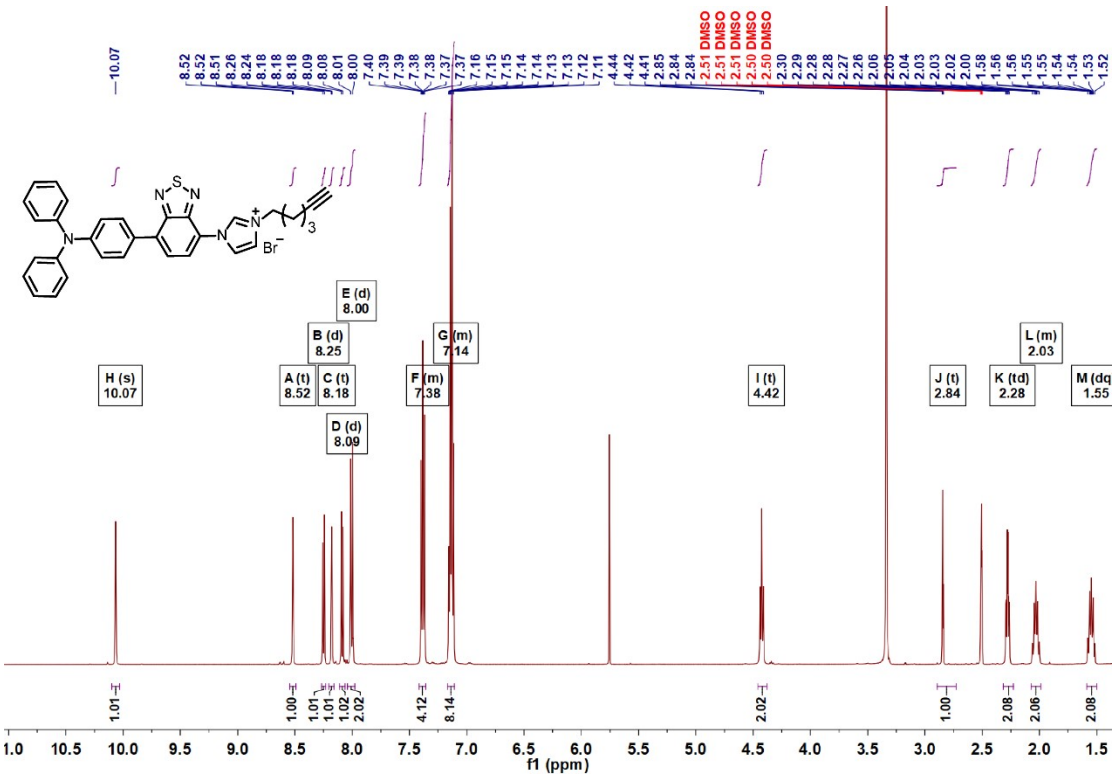

Figure S12. ^{1}H NMR spectrum of compound **T-CCH**.

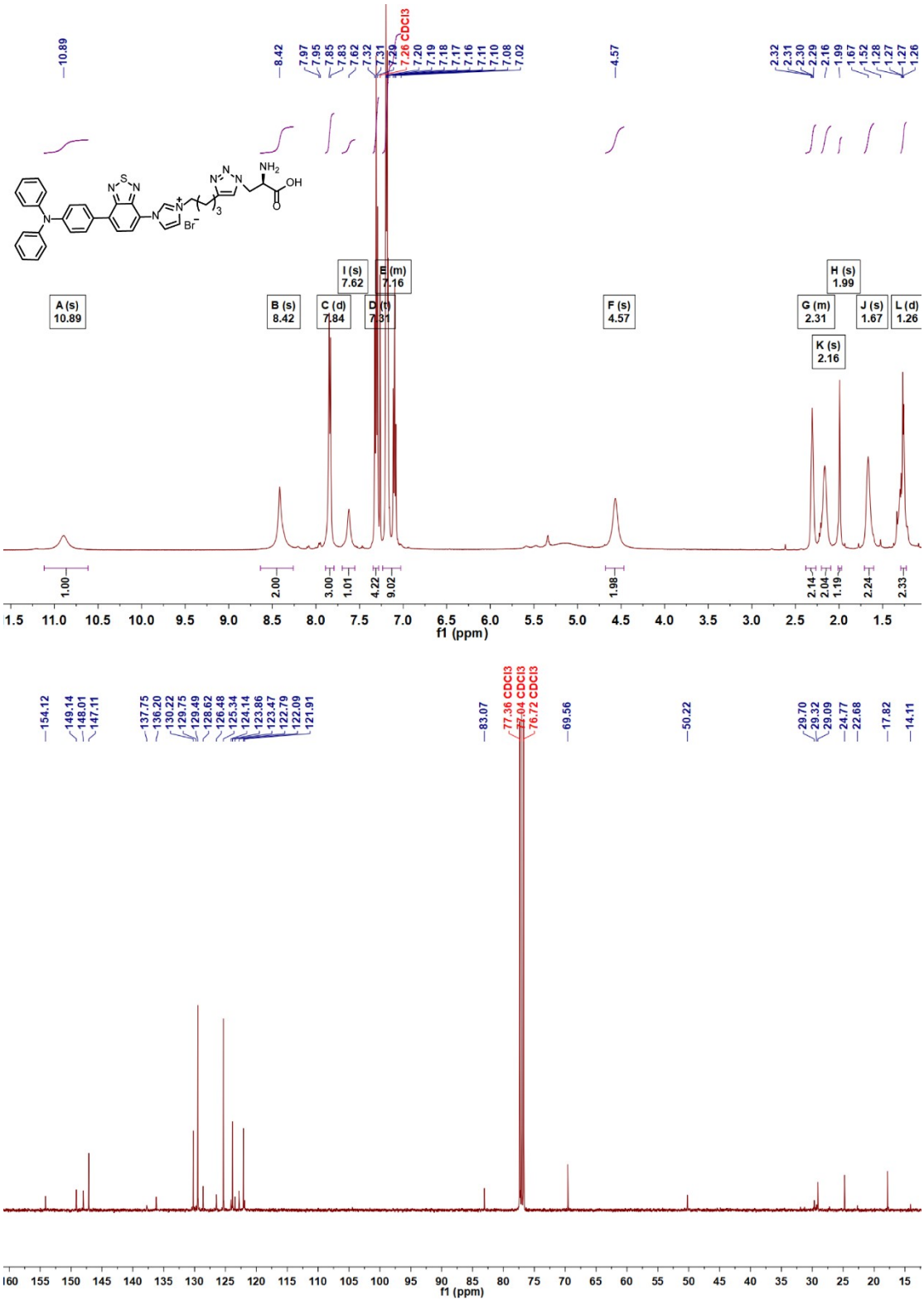

Figure S13. ^{1}H NMR and ^{13}C NMR spectrum of compound **T-DAla**.

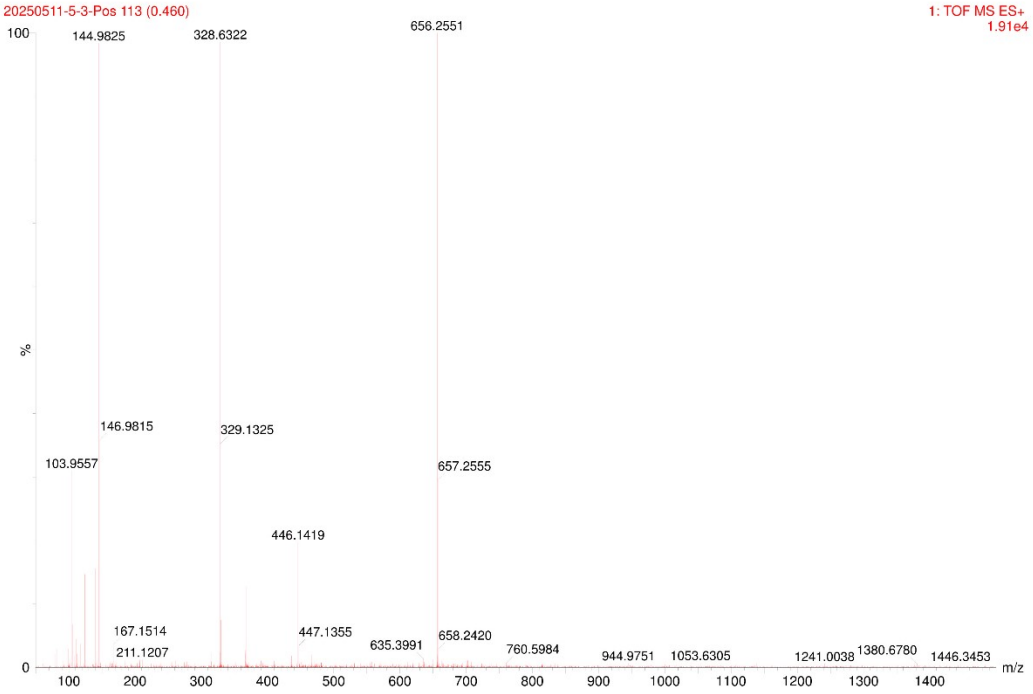

Figure S14. HRMS spectrum of compound **T-DAla**.

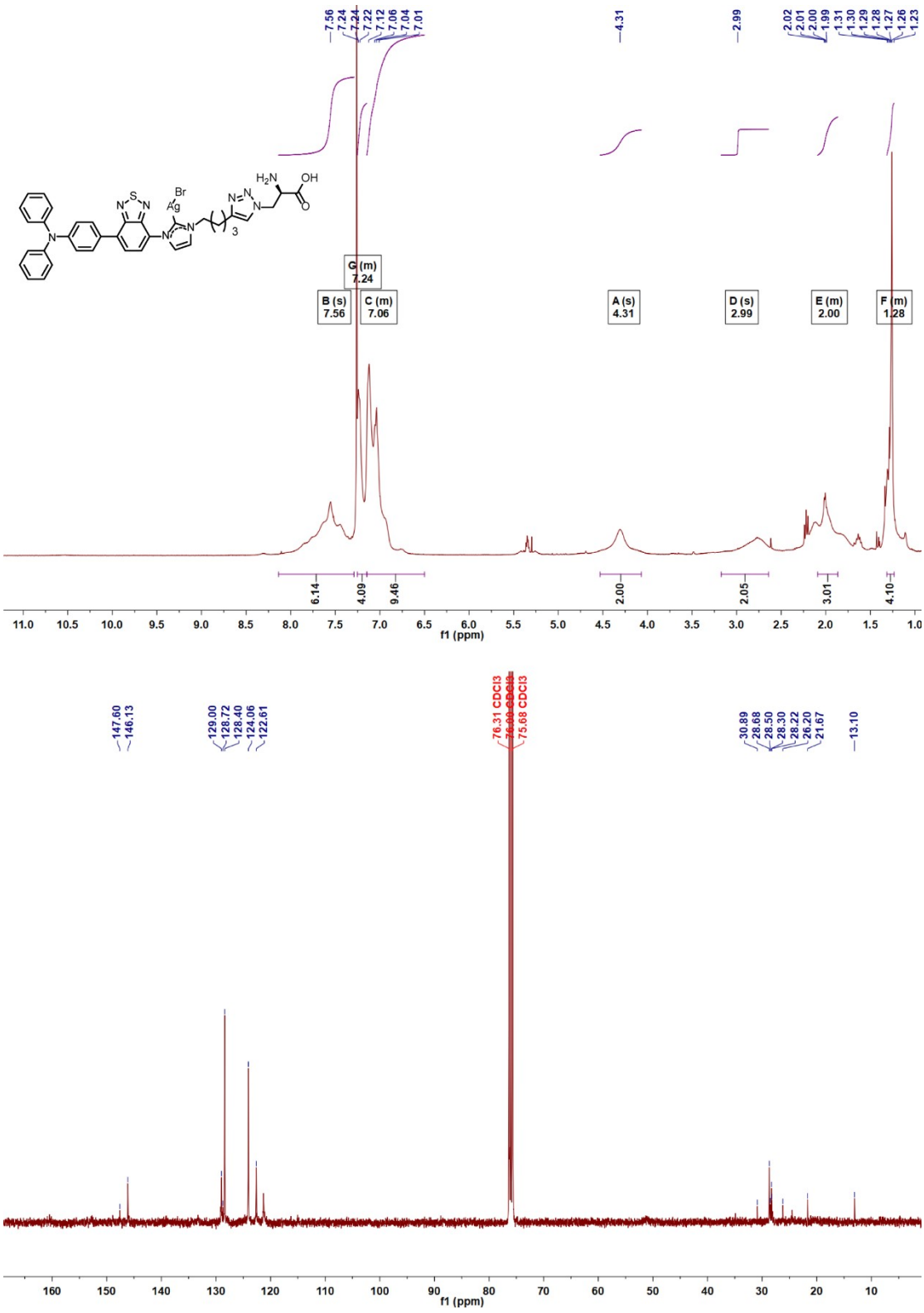

Figure S15. ^{1}H NMR and ^{13}C NMR spectrum of compound **T-DAla-Ag.**

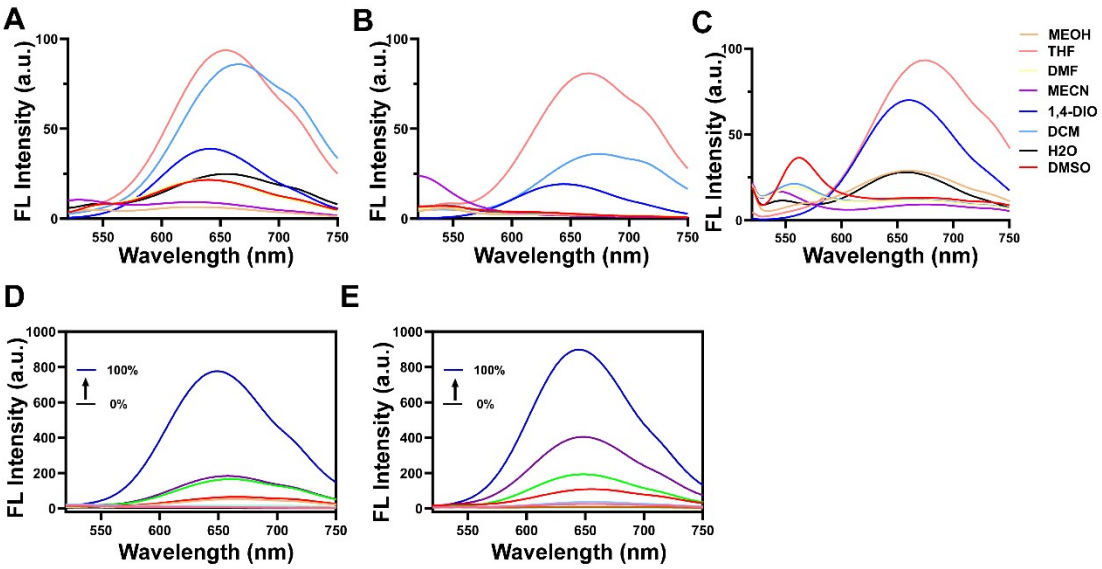

Figure S16. FL spectra of A) **T-C_{12}**, B) **T-BOB**, and C) **T-DAla** in different solutions. FL spectra of D) **T-C_{12}** and E) **T-BOB** in different fractions of H_2O/1,4-Dio mixture.

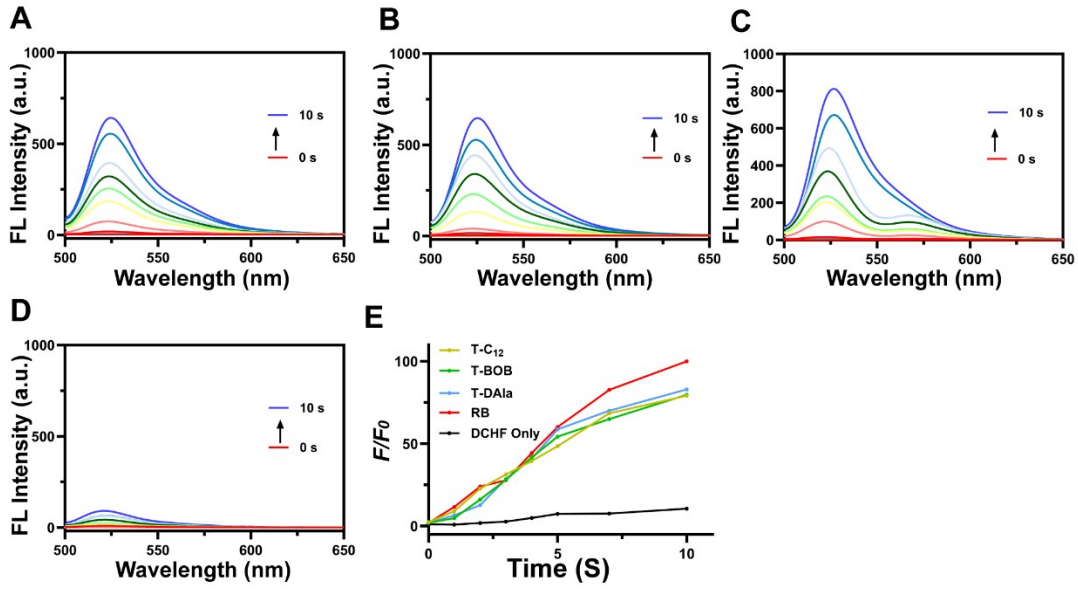

Figure S17. FL spectra of DCFH-DA with A) **T-C_{12}**, B) **T-BOB**, and C) RB and D) DCFH-DA only under white-light irradiation (60 mW cm^{-2}) at different time points. E) Relative fluorescence intensity (F/F_0) of DCFH at 522 nm.

Figure S18. Absorption spectra of ABDA with A) **T-C$_{12}$**, B) **T-BOB**, and C) RB and D) ABDA only under white-light irradiation (60 mW cm^{-2}) at different time points.

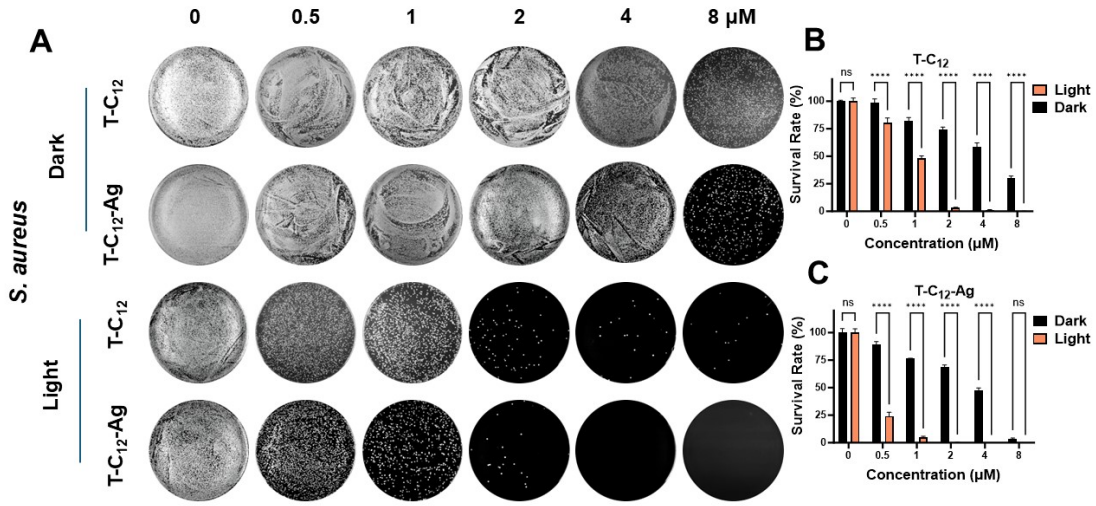

Figure S19. Agar plate photographs and quantitative analysis of survival rates (CFU-based) of *S. aureus* incubated with different concentrations of **T-C$_{12}$** or **T-C$_{12}$-Ag** for 20 min, with or without white-light irradiation for 15 min (60 mW cm^{-2}).

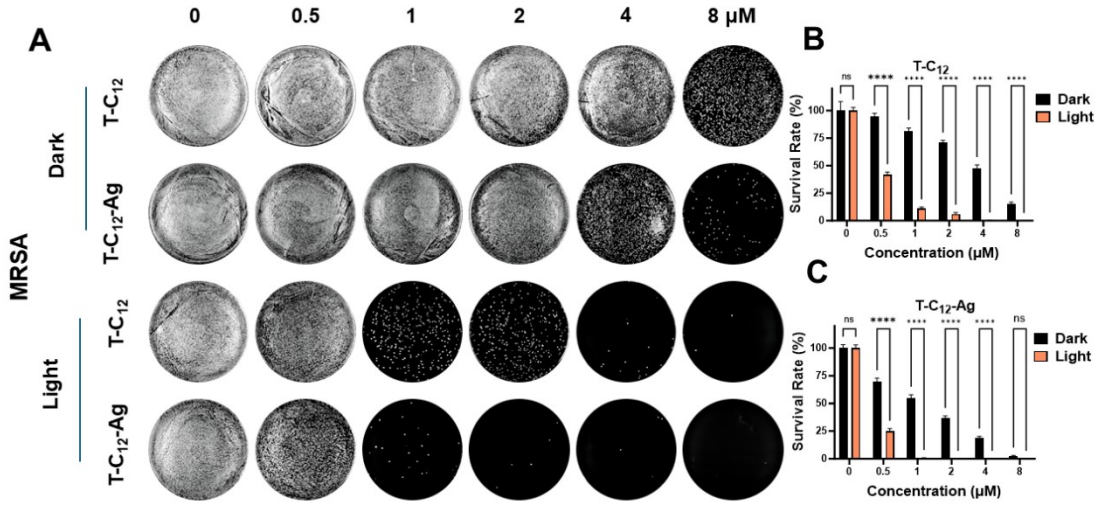

Figure S20. Agar plate photographs and quantitative analysis of survival rates (CFU-based) of MRSA incubated with different concentrations of **T-C$_{12}$** or **T-C$_{12}$-Ag** for 20 min, with or without white-light irradiation for 15 min (60 mW cm^{-2}).

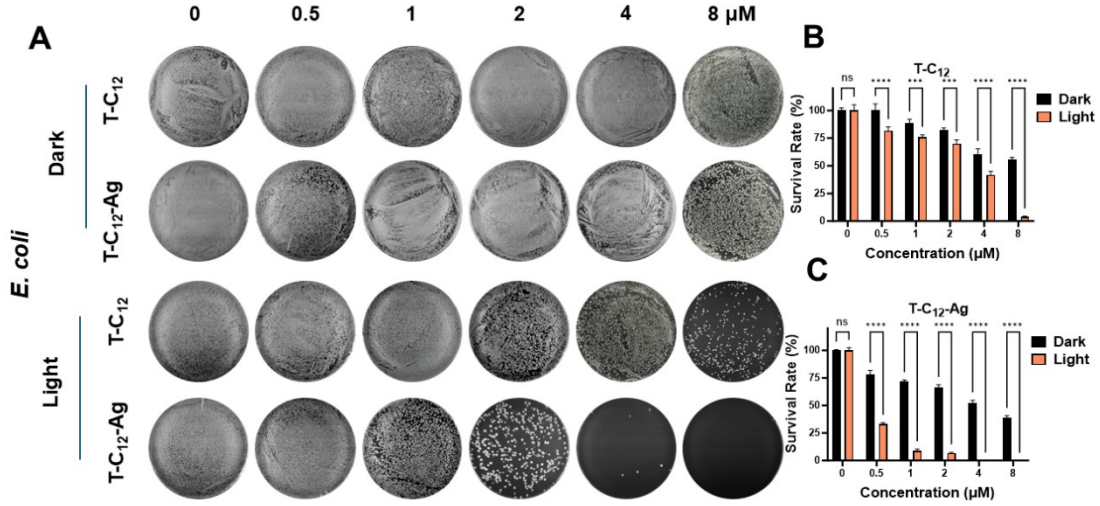

Figure S21. Agar plate photographs and quantitative analysis of survival rates (CFU-based) of *E. coli* incubated with different concentrations of **T-C$_{12}$** or **T-C$_{12}$-Ag** for 20 min, with or without white-light irradiation for 15 min (60 mW cm^{-2}).

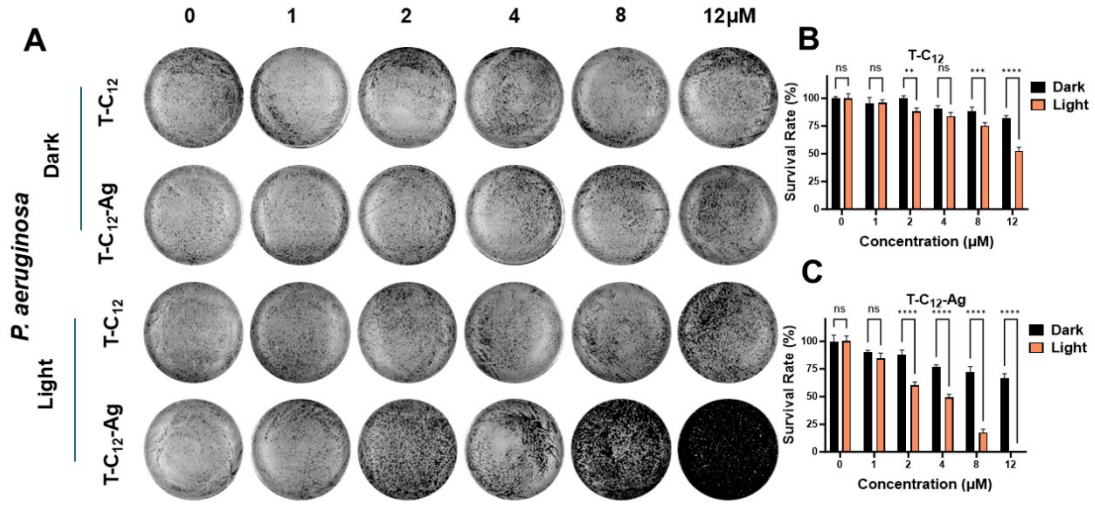

Figure S22. Agar plate photographs and quantitative analysis of survival rates (CFU-based) of *P. aeruginosa* incubated with different concentrations of **T-C_{12}** or **T-C_{12}-Ag** for 20 min, with or without white-light irradiation for 15 min (60 mW cm^{-2}).

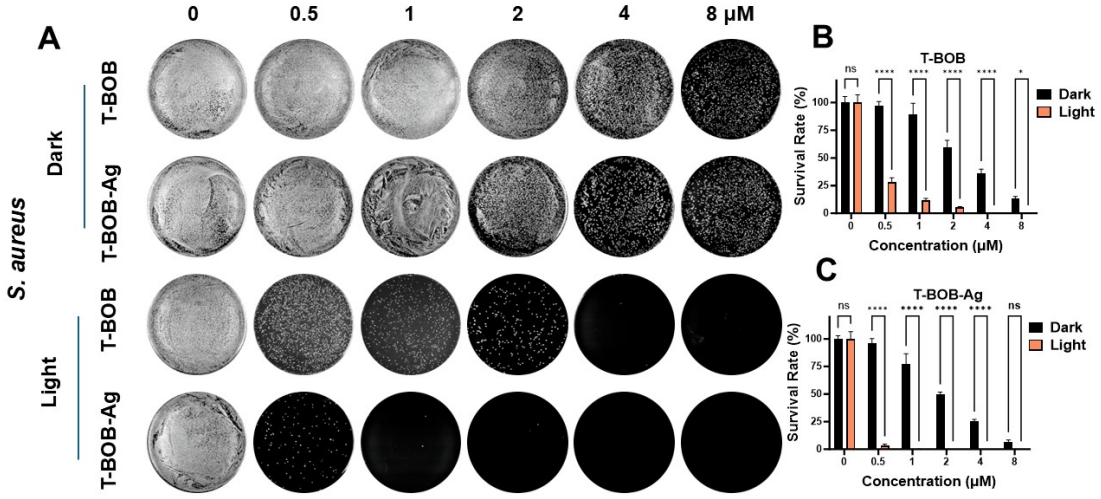

Figure S23. Agar plate photographs and quantitative analysis of survival rates (CFU-based) of *S. aureus* incubated with different concentrations of **T-BOB** or **T-BOB-Ag** for 20 min, with or without white-light irradiation for 15 min (60 mW cm^{-2}).

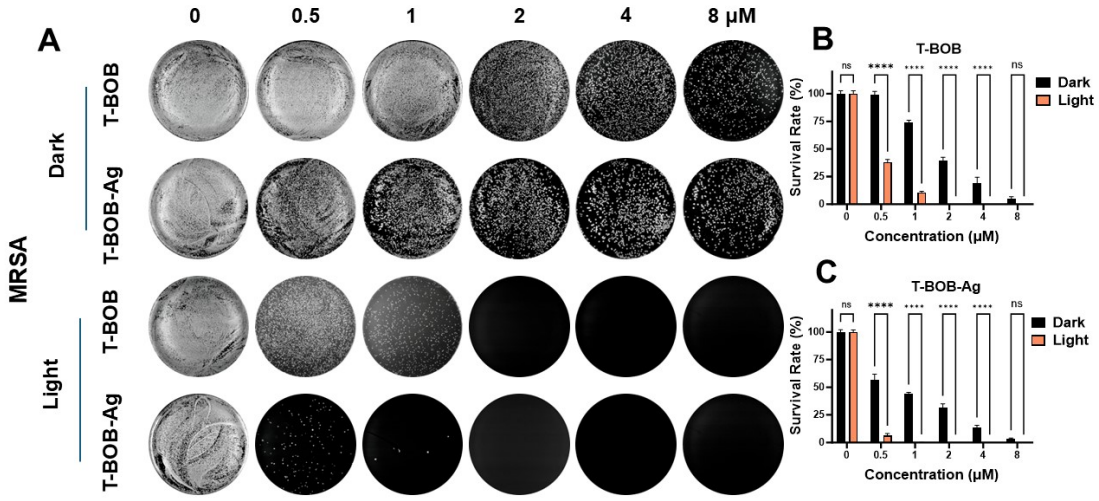

Figure S24. Agar plate photographs and quantitative analysis of survival rates (CFU-based) of MRSA incubated with different concentrations of **T-BOB** or **T-BOB-Ag** for 20 min, with or without white-light irradiation for 15 min (60 mW cm^{-2}).

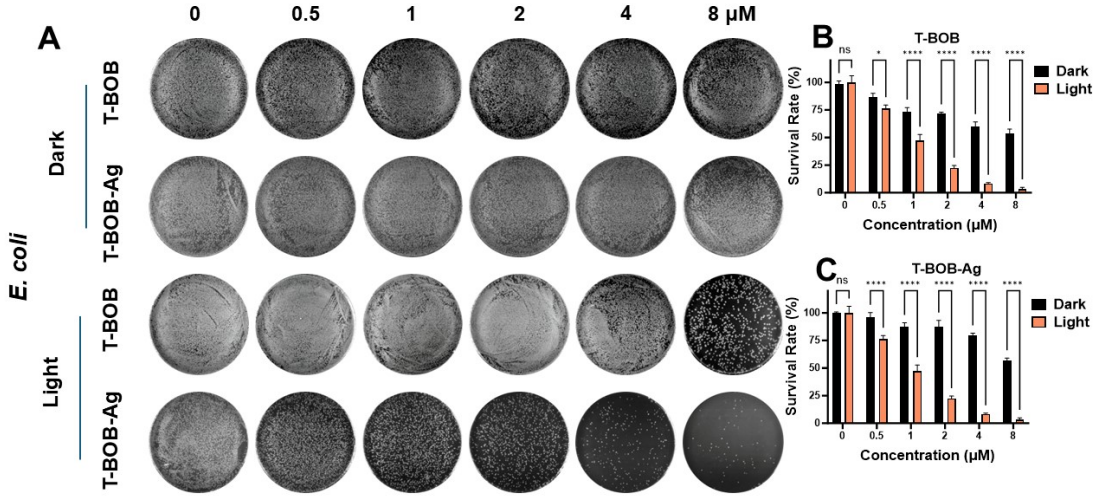

Figure S25. Agar plate photographs and quantitative analysis of survival rates (CFU-based) of *E. coli* incubated with different concentrations of **T-BOB** or **T-BOB-Ag** for 20 min, with or without white-light irradiation for 15 min (60 mW cm^{-2}).

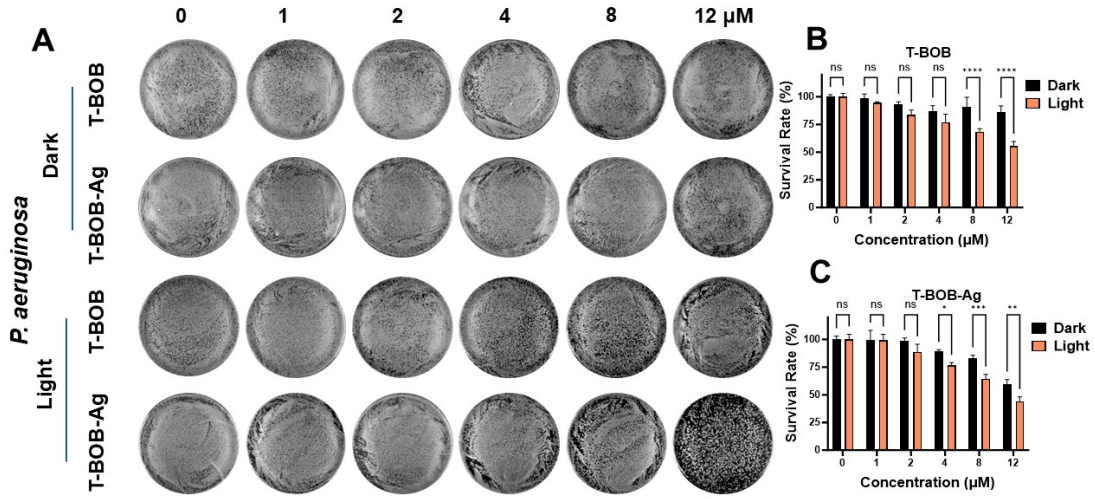

Figure S26. Agar plate photographs and quantitative analysis of survival rates (CFU-based) of *P. aeruginosa* incubated with different concentrations of **T-BOB** or **T-BOB-Ag** for 20 min, with or without white-light irradiation for 15 min (60 mW cm^{-2}).

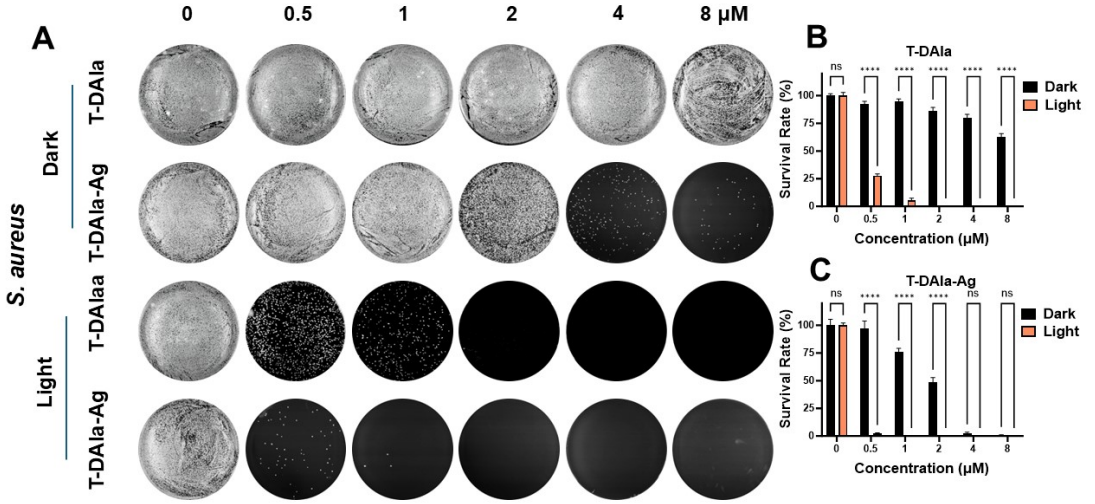

Figure S27. Agar plate photographs and quantitative analysis of survival rates (CFU-based) of *S. aureus* incubated with different concentrations of **T-DAla** or **T-DAla-Ag** for 20 min, with or without white-light irradiation for 15 min (60 mW cm^{-2}).

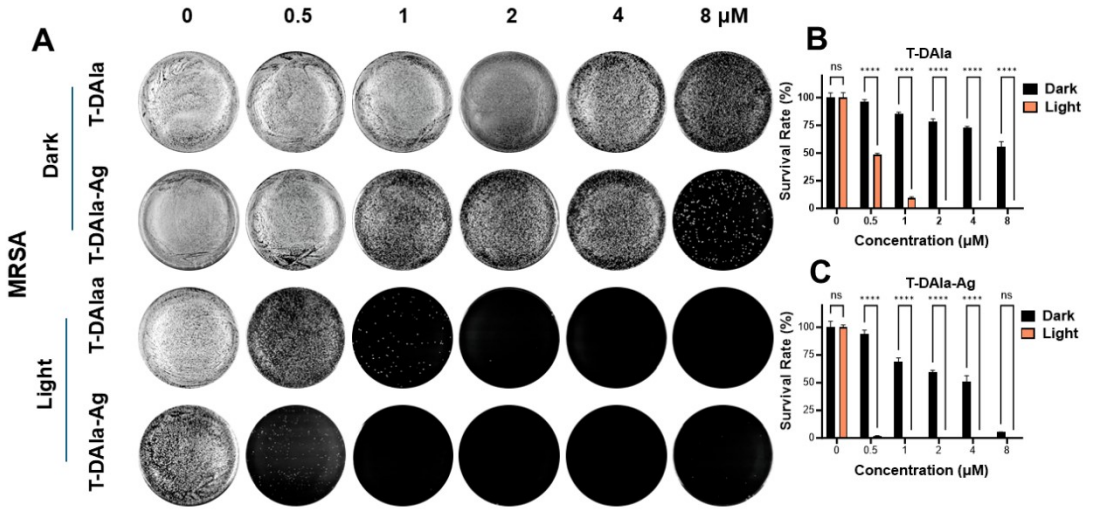

Figure S28. Agar plate photographs and quantitative analysis of survival rates (CFU-based) of MRSA incubated with different concentrations of **T-DAla** or **T-DAla-Ag** for 20 min, with or without white-light irradiation for 15 min (60 mW cm^{-2}).

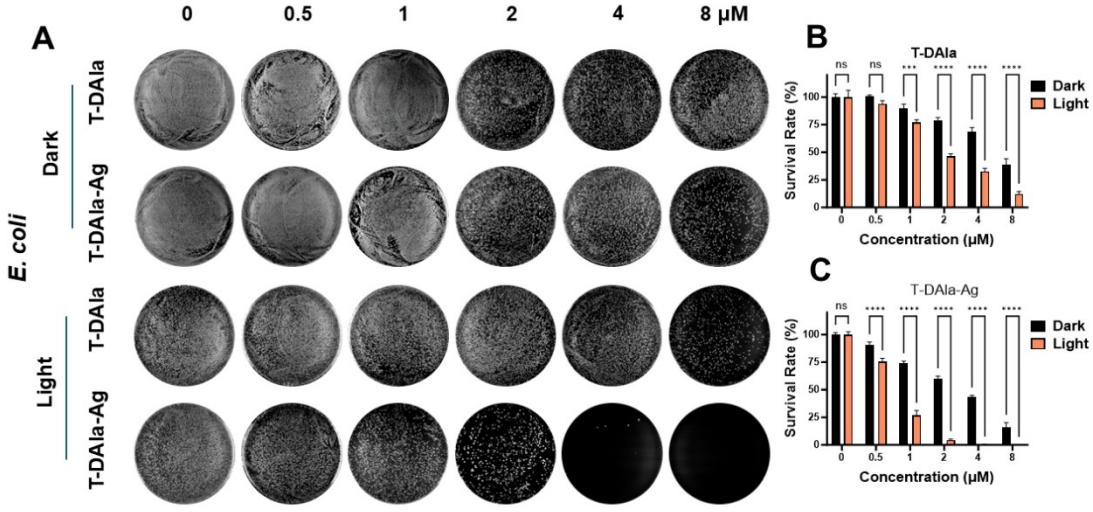

Figure S29. Agar plate photographs and quantitative analysis of survival rates (CFU-based) of *E. coli* incubated with different concentrations of **T-DAla** or **T-DAla-Ag** for 20 min, with or without white-light irradiation for 15 min (60 mW cm^{-2}).

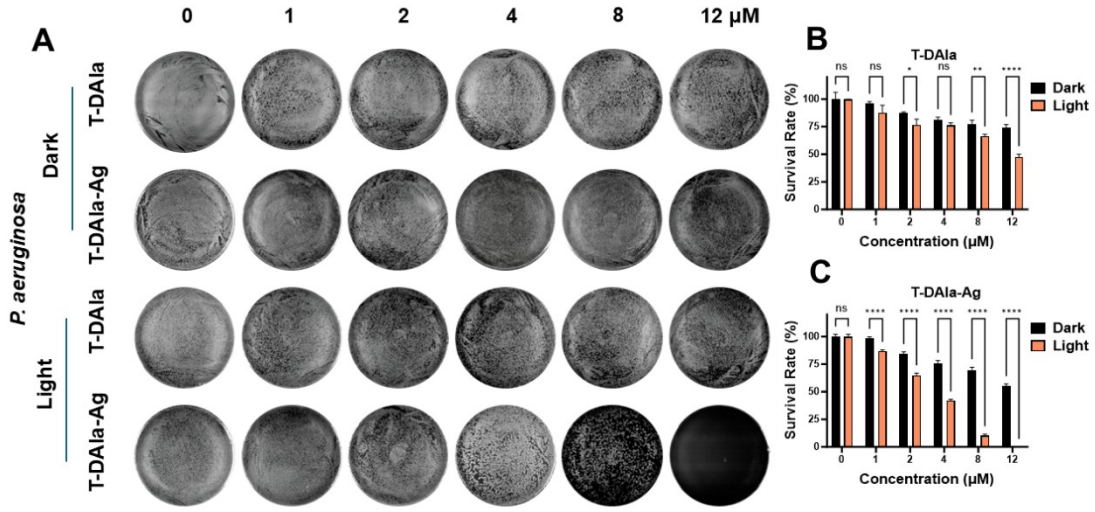

Figure S30. Agar plate photographs and quantitative analysis of survival rates (CFU-based) of *P. aeruginosa.* incubated with different concentrations of **T-DAla** or **T-DAla-Ag** for 20 min, with or without white-light irradiation for 15 min (60 mW cm^{-2}).

Table S1. CFU-based minimum inhibitory concentration (MIC) values of **T-C12**, **T-BOB**, **T-DAla**, and their Ag complexes under dark and light conditions against different bacterial strains.

Light-activated MICs (μM) of the tested compounds								
Sample	*S. aureus*		MRSA		*E. coli*		*P. aeruginosa*	
	Dark	Light	Dark	Light	Dark	Light	Dark	Light
T-C_{12}	>8	8	>8	8	>8	>8	>12	>12
T-BOB	>8	4	>8	2	>8	>8	>12	>12
T-DAla	>8	2	>8	2	>8	>8	>12	>12
T-C_{12}-Ag	>8	4	>8	8	>8	8	>12	>12
T-BOB-Ag	>8	2	>8	2	>8	>8	>12	>12
T-DAla-Ag	>8	2	>8	1	>8	8	>12	12

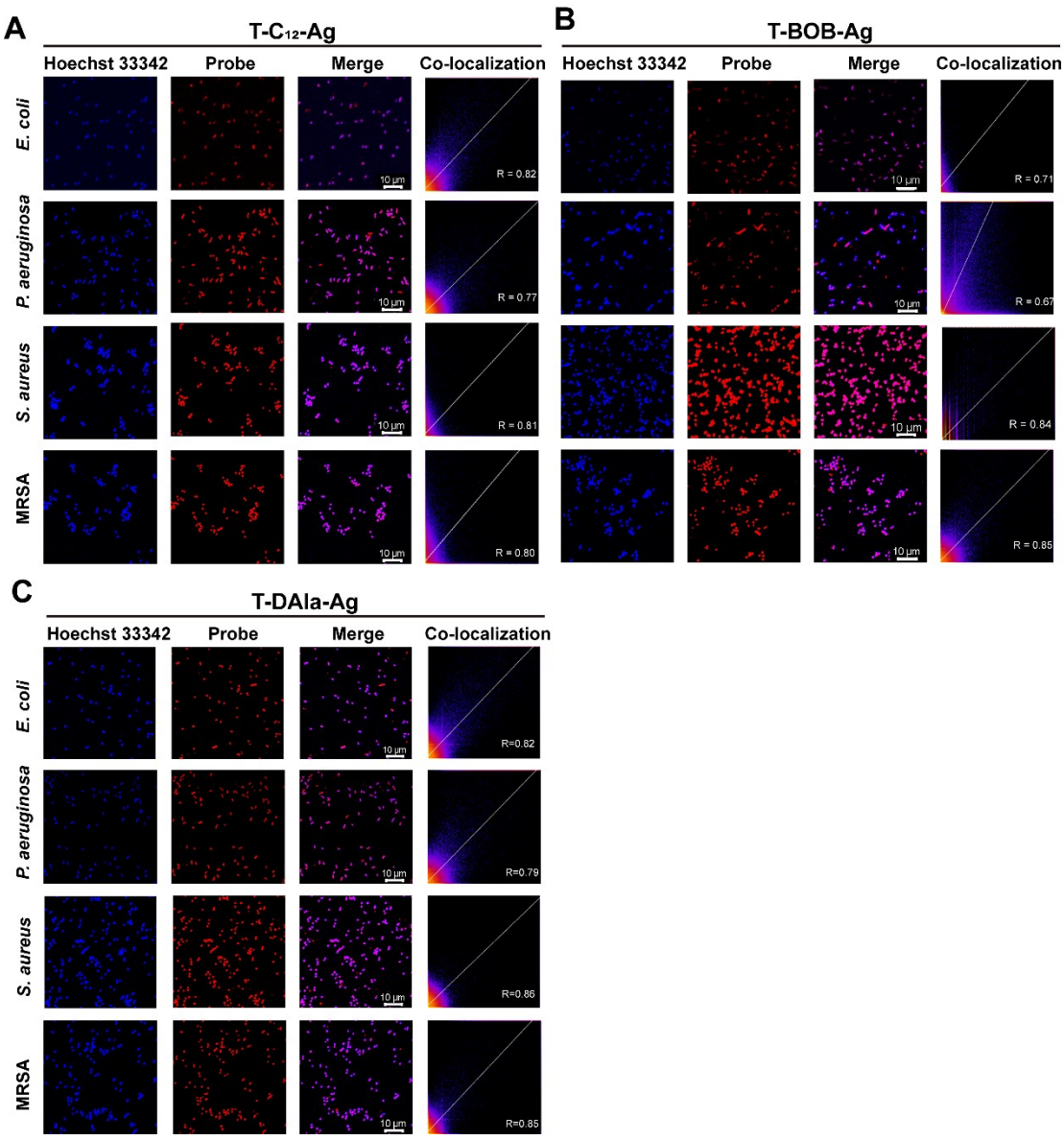

Figure S31. CLSM images of *E. coli*, *P. aeruginosa*, *S. aureus*, and MRSA after incubation with (A) **T-C_{12}-Ag** (10 μM), (B) **T-BOB-Ag** (10 μM) and (C) **T-DAla-Ag** (10 μM) followed by co-staining with Hoechst 33342 for 15 min. Scale bar: 10 μm.

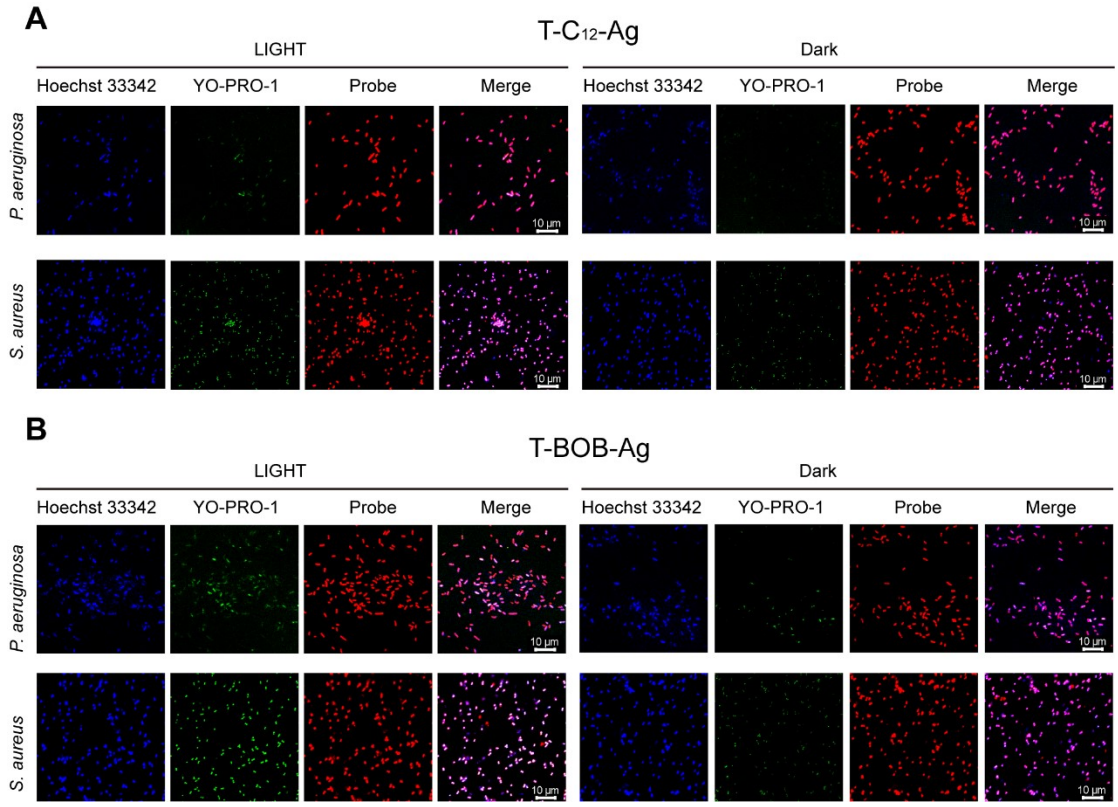

Figure S32. CLSM images of *S. aureus* upon incubation with (A) **T-C_{12}-Ag** (10 μM) and (B) **T-BOB-Ag** (10 μM) for 30 min and then without or with white-light (60 mW cm^{-2}) irradiation for 30 min. Then co-staining with Hoechst 33342 and YO-PRO-1 for 15 min. Scale bar: 10 μm.

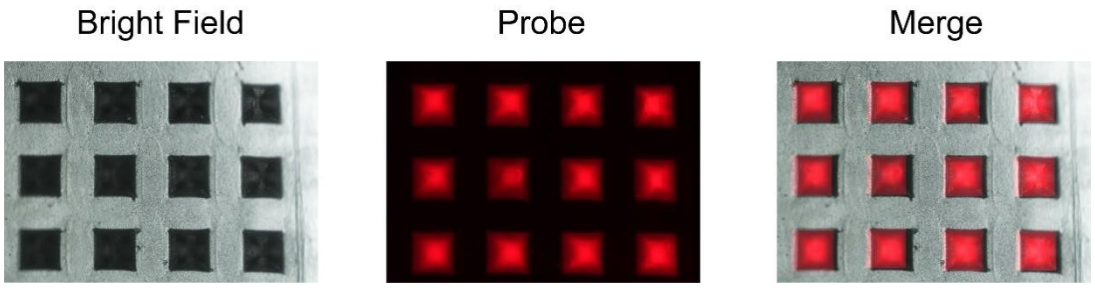

Figure S33. Optical microscope images of the **Probe@DMN**, T-DAla-Ag loaded PVP K30 core (red fluorescence)

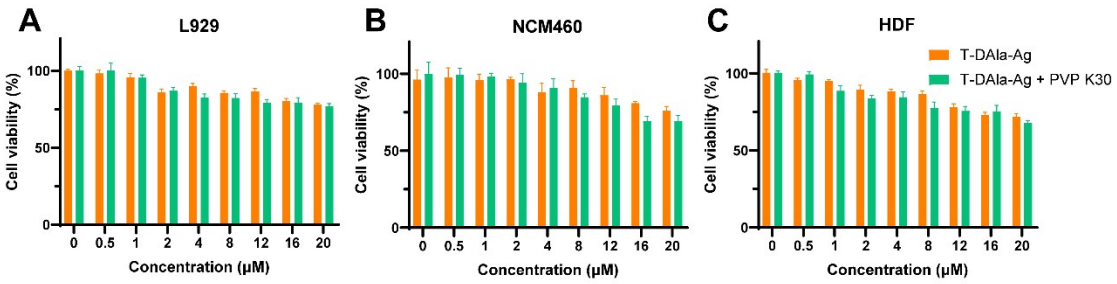

Figure S34. Cell viabilities of A) L929 cells, B) NCM460 cells and C) HDF cells treated with different concentrations of **T-DAla-Ag** or **T-DAla-Ag** + PVP K30.

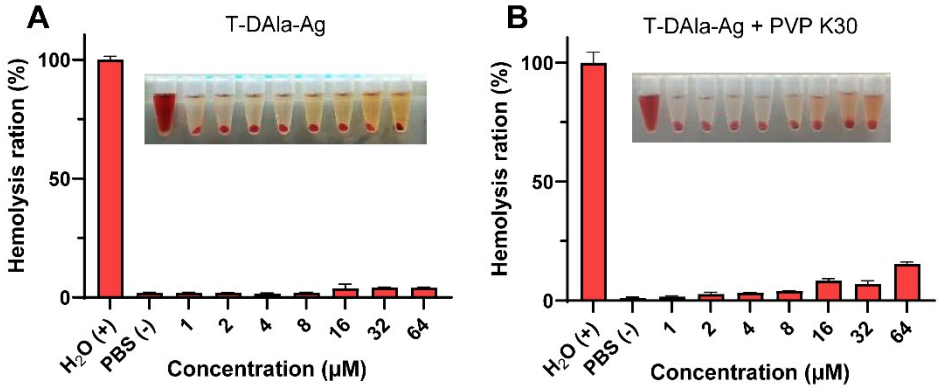

Figure S35. Hemolysis assay of **T-DAla-Ag** or **T-DAla-Ag** + PVP K30. No hemolytic effect was observed with red blood cells after being treated with **T-DAla-Ag** or **T-DAla-Ag** + PVP K30 at varying concentrations from 1 to 64 μM, using H_2O as a positive control and saline as a negative control.

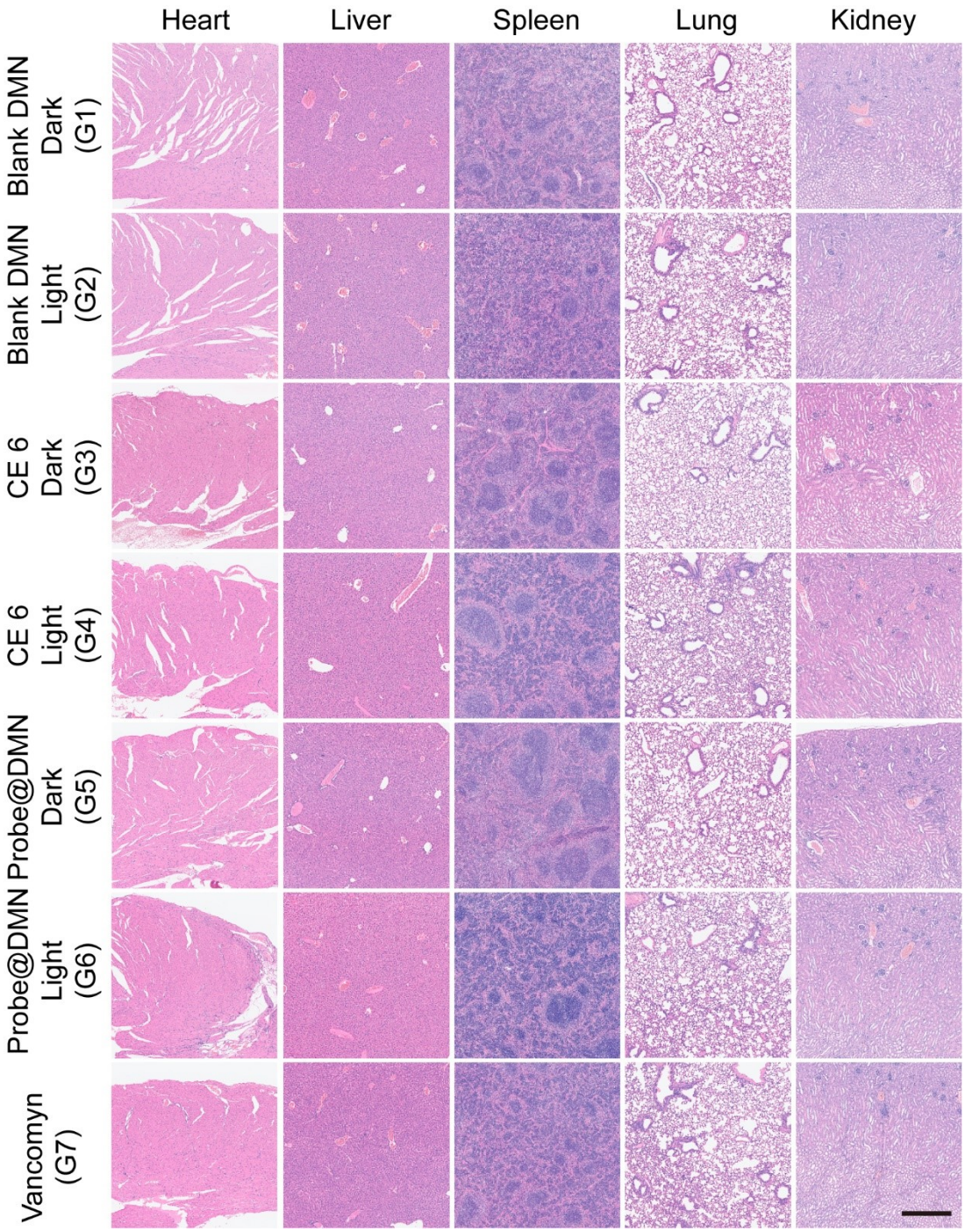

Figure S36. Histological H&E staining images of heart, liver, spleen, lung and kidney collected on day 14 from different groups. Scale bar: 500 μm.

Table S2. Theoretical and experimental Ag contents of **T-C_{12}-Ag**, **T-BOB-Ag**, and **T-DAla-Ag** determined by ICP-OES, expressed as weight percentage (wt%).

Sample	Theoretical Ag (wt%)	Experimental Ag (wt%)	Ag Incorporation Efficiency (%)
T-C_{12}-Ag	13.37	10.56	78.76

T-BOB-Ag	12.07	7.86	65.15
T-DAla-Ag	12.77	10.75	84.23

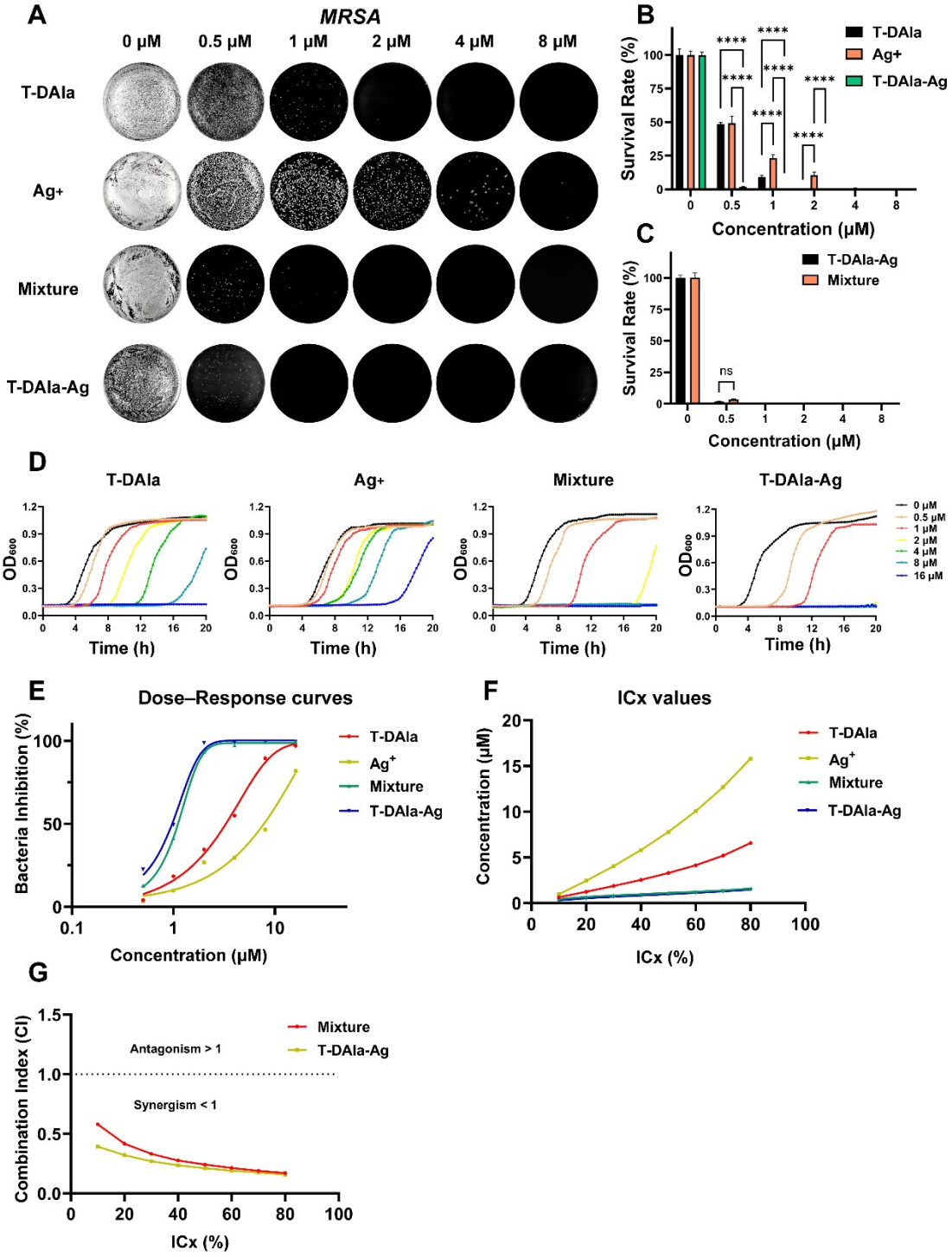

Figure S37. Evaluation of the synergistic antibacterial effect of Ag in organic silver photosensitizers. (A) Representative colony formation images of MRSA treated with **T-DAla**, Ag_+, mixture (1:1), and **T-DAla-Ag** at different concentrations. (B) Quantitative analysis of bacterial survival rates under different treatments. (C)

Comparison of antibacterial activity between the mixture and **T-DAla-Ag**. (D) Bacterial growth curves of MRSA treated with increasing concentrations of different formulations. (E) Dose–response curves showing bacterial inhibition as a function of concentration. (F) IC_x values derived from the fitted dose–response curves, representing the concentrations required to achieve different inhibition levels (IC_{10}–IC_{80}). (G) Combination index (CI) values of the mixture and **T-DAla-Ag** at different effect levels. The dashed line at CI = 1 indicates an additive effect; CI < 1 indicates synergism, while CI > 1 indicates antagonism.

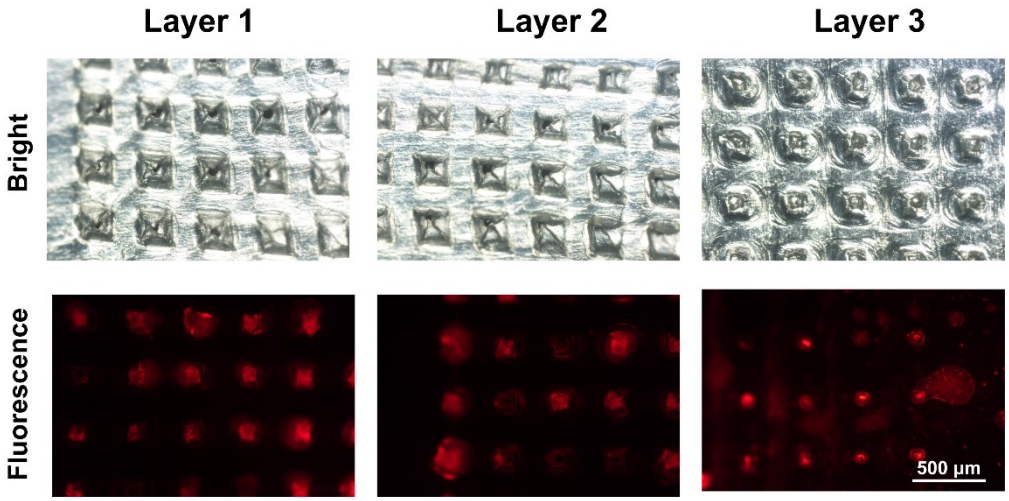

Figure S38. Evaluation of microneedle insertion capability using a multilayer Parafilm model. Bright-field images (top row) show the formation of distinct micro-holes in Parafilm layers (Layer 1–3) after microneedle application. Fluorescence images (bottom row) were obtained after dye administration, where the red fluorescence indicates successful penetration and dye deposition at the insertion sites across different layers. These results confirm that the fabricated microneedles possess sufficient insertion capability to penetrate multiple layers. Scale bar: 500 μm.